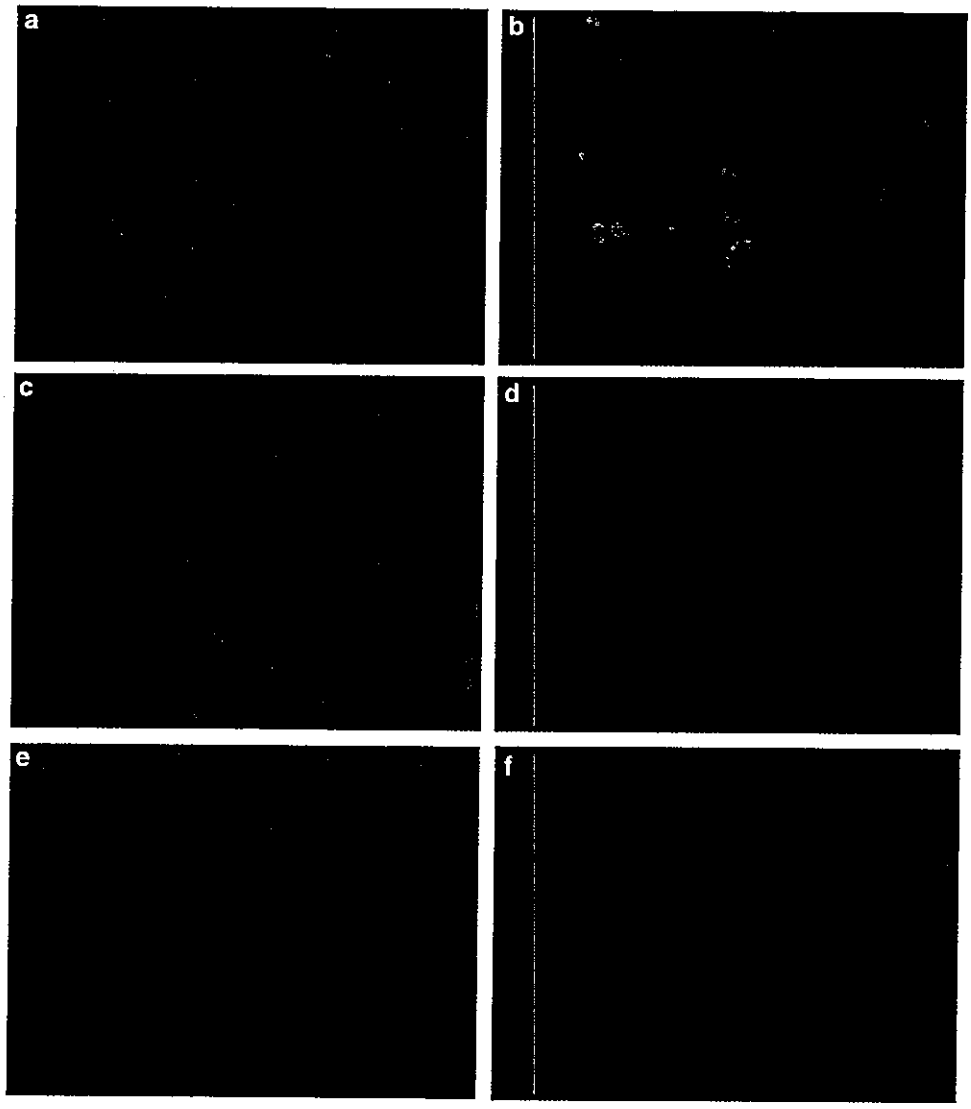

Figure 3 TUNEL staining. U251 cells were infected with AVC2-BimS (a, b), AVC2-BimL (c, d), or AVC2-tk (e, f) at an MOI of 20. Thirty-six hours later, cells were fixed and subjected to TUNEL analysis, followed by Evans blue staining. Evans blue staining (a, c, e) and TUNEL staining (b, d, f) were visualized by fluorescence microscopy.

Enhancement of the anti-tumor effect of tk/GCV treatment by BimS in an animal model

The encouraging results described above prompted us to perform experiments in an animal model to test the potential of BimS for enhancing the performance of HSV-tk/GCV therapy. U251 cells (4×10^6) were inoculated subcutaneously into nude mice together with AVC2-BimS, AVC2-BimL, AVC2-tk, or AVC2-LacZ adenovirus vectors, which were injected either as a sole vector or in combination. When a single injection of AVC2-BimL, AVC2-LacZ, or AVC2-tk (followed by i.p. injections of PBS) was administered to the tumor, continuous tumor growth was observed (Figure 6a). Injection of adenovirus vectors containing either AVC2-BimS or AVC2-tk (followed by i.p. injections of GCV) checked tumor growth temporarily, but eventually the tumor began to regrow. As expected, the combination treatment with AVC2-BimS and AVC2-tk (followed by i.p. injections of GCV) inhibited tumor regrowth.

To test the joint effect of tk/GCV and BimS treatment in animal model, we applied the growth curve model (eg Potthoff and Roy[25]) for the tumor growth data. The response is 'logarithmic transformed tumor size', the time variable is 'Days after treatment', and nine treatments are used as the class variables. For every treatment group, a quadratic growth curve is fitted through the least-squares method (Figure 6b). Then a set of the null hypotheses about effects of 'tk/GCV+BimS', 'tk/GCV', and 'BimS', which we are interested in, were listed in the table. The estimated coefficients for the above three treatments were statistically compared by Wald-type T^2 statistic that is subject to Chi-squared distribution asymptotically under the null hypothesis.[26] The results showed that all of the null hypotheses were rejected with high significance levels ($P<0.01$), indicating that the strong joint effect of 'tk/GCV+BimS' compared with the expected additive effect of 'tk/GCV' and 'BimS'.

To confirm that BimS induced apoptosis in tumor cells in this animal model, expression of BimS and

Table 1 Results of null hypothesis tests

Hypothesis	*Degree of freedom*	*T2 statistic*	*P-value*
T1=T2=T3	6	45.5	0.00
T1=T2	3	9.92	0.02
T1=T3	3	40.0	0.00

T1: tk/GCV+BimS; T2: tk/GCV; T3: BimS.

DNA fragmentation was analyzed using immunohistochemical analysis and TUNEL assay. Before infection by AVC2-BimS, U251 cells looked healthy with relatively low-level expression of Bim protein in cytoplasm (Figure 7a), because the tumor cells expressed BimEL and BimL (Figure 1a, lane 2) and the affinity-purified Bim antibody used in this study recognizes all three forms of Bim protein. Three days after infection, we

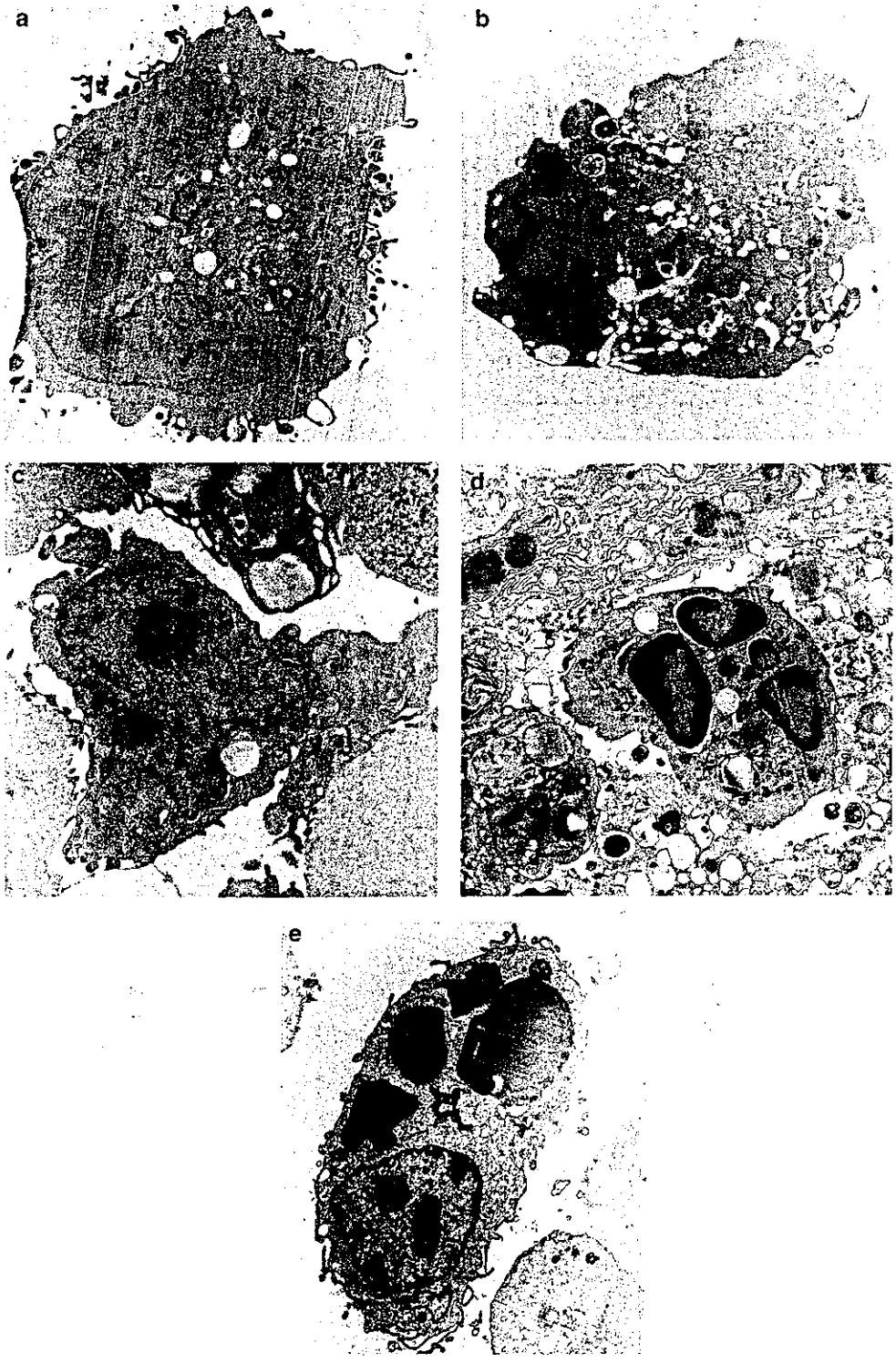

Figure 4 Electron micrographs of U251 cells before (a, c) and after infection by AVC2-BimS (b, d, e) in vitro (a, b) or in animal model (c–e).

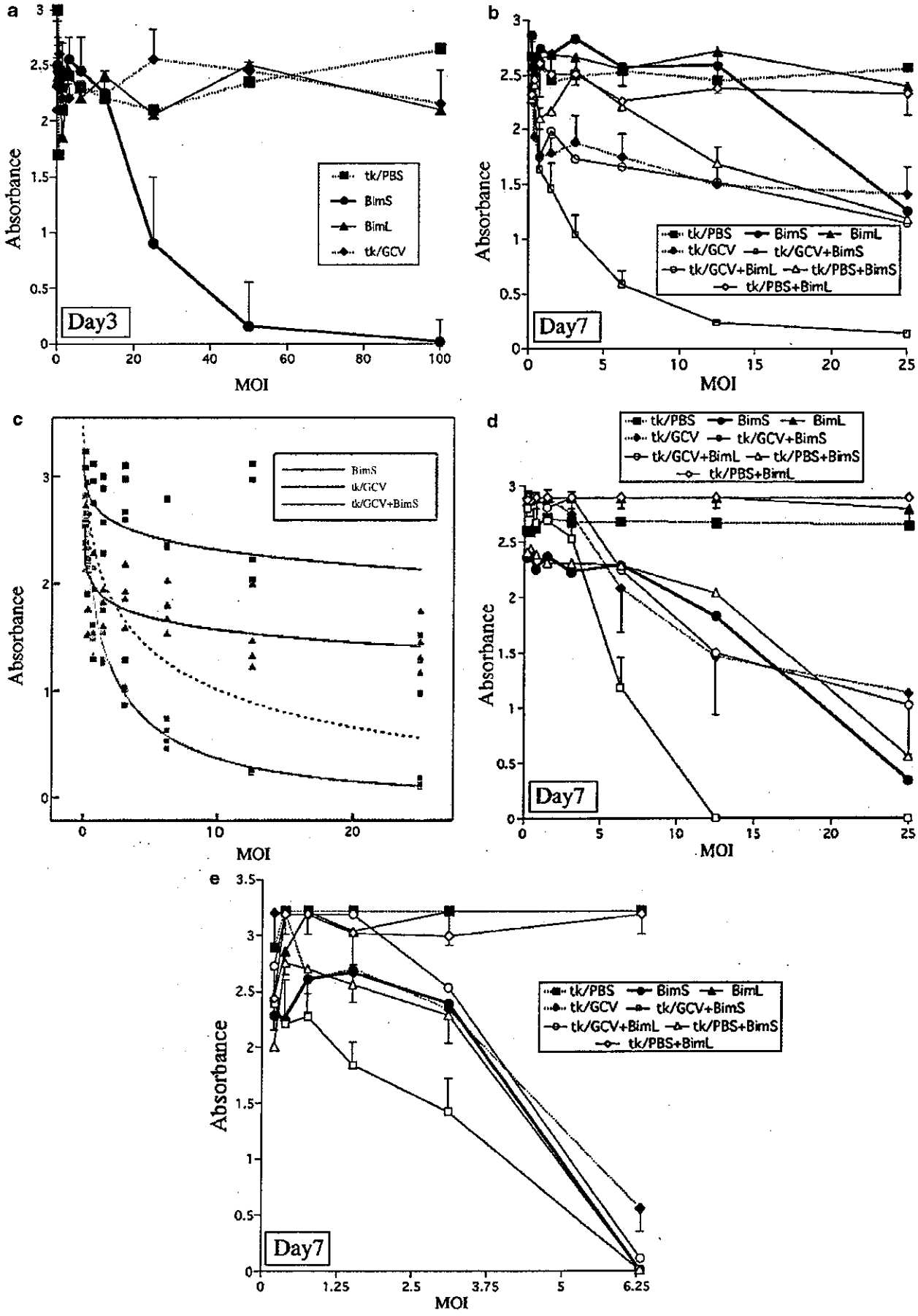
a
Absorbance
MOI
tk/PBS
BimS
BimL
tk/GCV
Day3
b
Absorbance
MOI
tk/PBS
BimS
BimL
tk/GCV
tk/GCV+BimS
tk/GCV+BimL
tk/PBS+BimS
tk/PBS+BimL
Day7
c
Absorbance
MOI
BimS
tk/GCV
tk/GCV+BimS
d
Absorbance
MOI
tk/PBS
BimS
BimL
tk/GCV
tk/GCV+BimS
tk/GCV+BimL
tk/PBS+BimS
tk/PBS+BimL
Day7
e
Absorbance
MOI
tk/PBS
BimS
BimL
tk/GCV
tk/GCV+BimS
tk/GCV+BimL
tk/PBS+BimS
tk/PBS+BimL
Day7

observed that tumor cells expressing Bim proteins at high levels had TUNEL-positive shrunken nuclei (Figure 7b, arrowheads). In contrast, cells expressing Bim at background levels had TUNEL-negative healthy nuclei (arrows), suggesting that BimS induced apoptosis in U251 cells also in the animal model. Induction of apoptosis by BimS was again confirmed by electron microscopy. Three days after infection by AVC2-BimS, cells carrying fragmented nuclei with condensed chromatin were readily found (Figure 4d) and apoptotic bodies phagocytosed by surrounding cells were observed (Figure 4e).

Discussion

In this paper, we transferred the BH3-only death activator genes, BimL and BimS, to malignant glioma cells using adenovirus vectors in an attempt to enhance HSV-tk/GCV-mediated killing *in vitro* and *in vivo*. Using 293B cells that overexpressed Bcl-x_L, we were able to protect virus-producing cells from apoptosis induced by Bim and obtained high titers of adenovirus stocks that were capable of transferring genes into tumors in nude mice. BimS, but not BimL, induced rapid apoptosis in malignant glioma cells, in spite of the fact that BimL seemed to be expressed at higher levels than BimS as determined by immunoblot analysis (Figure 2b). In the case of the 293 cells, however, both variants of Bim equally induced cell death.

Bim is controlled by several mechanisms. First, its expression levels are regulated by cytokines and neurotrophic factors through Ras and PI3-K pathways in hematopoietic cells[11,17] and in neurons.[19] Bim is also phosphorylated by cytokine-initiating signal pathways, although it is not known whether the phosphorylation of Bim regulates its function.[11] In addition, the subcellular localization of Bim protein was reported to be regulated by cytokines.[24] BimEL and BimL, but not BimS protein, form a complex with an M_r=8000 dynein light chain, LC8 (also PIN or Dlc-1),[22,23] which is a component of the dynein motor complex. In healthy cells, the Bim/LC8 complex binds to the intermediate chain of the dynein motor complex on the microtubules, which is physically separated from anti-apoptotic Bcl-2 family members on the surface of mitochondria. Apoptotic triggers dissociate the Bim/LC8 complex from the dynein intermediate chain by still undetermined mechanisms, enabling Bim to bind to antiapoptotic Bcl-2 family members and inhibit their function. The contribution of these three mechanisms to the regulation of Bim function is likely to be different in different cells. For instance, among murine interleukin (IL)-3-dependent cell lines, IL-3 starvation does not affect the expression levels of Bim proteins in FDC-P1 cells, while its subcellular distribution is regulated by IL-3 through the LC8-dependent mechanism.[24] In contrast, Bim proteins are induced by IL-3 withdrawal in Baf-3 and FL5.12 cells.[11,17] Moreover, forced (but not over) expression of BimEL or BimL readily induced apoptosis in Baf-3 cells even in the presence of IL-3,[17] suggesting that the expression levels of Bim proteins are critical for determining the fate of Baf-3 cells. These findings may help to explain the apparent differences in responsiveness to BimL in 293 and U251 cells.

BimS markedly enhanced the cytotoxic effect of tk/GCV therapy. In our animal model, although BimS and tk/GCV therapy reduced tumor volume rapidly, surviving cells eventually regrew (Figures 6a and b). Indeed, 3 days after infection, we observed tumor cells that expressed Bim protein at low levels and had healthy-looking nuclei (Figure 7b). These cells may be more efficiently eliminated by the combination of BimS and tk/GCV therapy than BimS alone. This synergistic effect is unlikely due to Bim's ability to induce cell death in a cell cycle phase independent fashion,[27] because we also observed this effect in *in vitro* experiments (Figure 5), where almost all cells were proliferating. Although we do not know the precise mechanism of this effect, it is possible that the simultaneous expression of BimS, which is the downstream target of growth factors/Ras-PI3-K pathways, and Bax (or other proapoptotic Bcl-2 family members) induced by HSV-tk/GCV treatment, served to enhance their respective cytotoxic potentials in the process by which they integrate their fate-determining signals. Alternatively, rapid induction of apoptosis in glioma cells by BimS may somehow have enhanced the cytotoxicity of HSV-tk/GCV therapy in the later phase. Recent studies suggested the possibility that gene products in cells undergoing apoptosis can be transferred from one tumor cell to another in the process of apoptosis,[28] since apoptotic bodies can be phagocytosed not only by macrophages but also by tumor cells.[29,30] Thus, HSV-tk protein expressed in cells infected by both AVC2-BimS and AVC2-tk might be transferred to neighboring tumor cells through phagocytosis and render these cells sensitive to GCV. We are currently investigating the molecular mechanism through which BimS enhances the cytotoxicity of HSV-tk/GCV therapy.

Cell cycle-independent induction of apoptosis by BimS may be useful in improving the efficacy of HSV-tk/GCV as a treatment of human disease by killing resting tumor cells, since the mitotic index in human malignant gliomas is much lower than that in animal models.[31] However, such treatment is likely to damage normal brain tissue including neurons. To avoid this problem, we attempted to express Bim protein using promoters of genes specifically expressed in malignant glioma cells but not in neurons, such as glial fibrillary acidic protein (GFAP)[32,33] or myelin basic protein (MBP),[34,35] but we were unable to obtain sufficient expression of Bim to induce cell death (data not shown). Development of a powerful glioma-specific promoter along with a tumor targeting vector system would be another key step to the application of this therapeutic approach in humans.

Figure 5 Analysis of cytotoxic effect using XTT assay. U251 (a, b), U373 (d), or T-430 cells (e) were infected with adenovirus vectors shown in insets at the various MOIs indicated below. In the case of AVC2-tk infection, either GCV (tk/GCV) or PBS (tk/PBS) was added to the culture medium after 48 h of infection. The XTT assay was performed on day 3 (a) or day 7 (b, d, e). Average absorbance ($A_{492\ nm}-A_{690\ nm}$) for each treatment and standard deviation for BimS and tk/GCV (a, d, e) or for BimL, tk/GCV, and tk/GCV+BimS (b) of four independent experiments were shown. (c) Statistical analysis of XTT assay using U251 cells at day 7. Fitted curves for each treatment indicated in a inset (solid lines) under no restriction and for tk/GCV+BimS treatment under H_0 (dotted line) in an original scale of y_{ij} and d_j were shown.

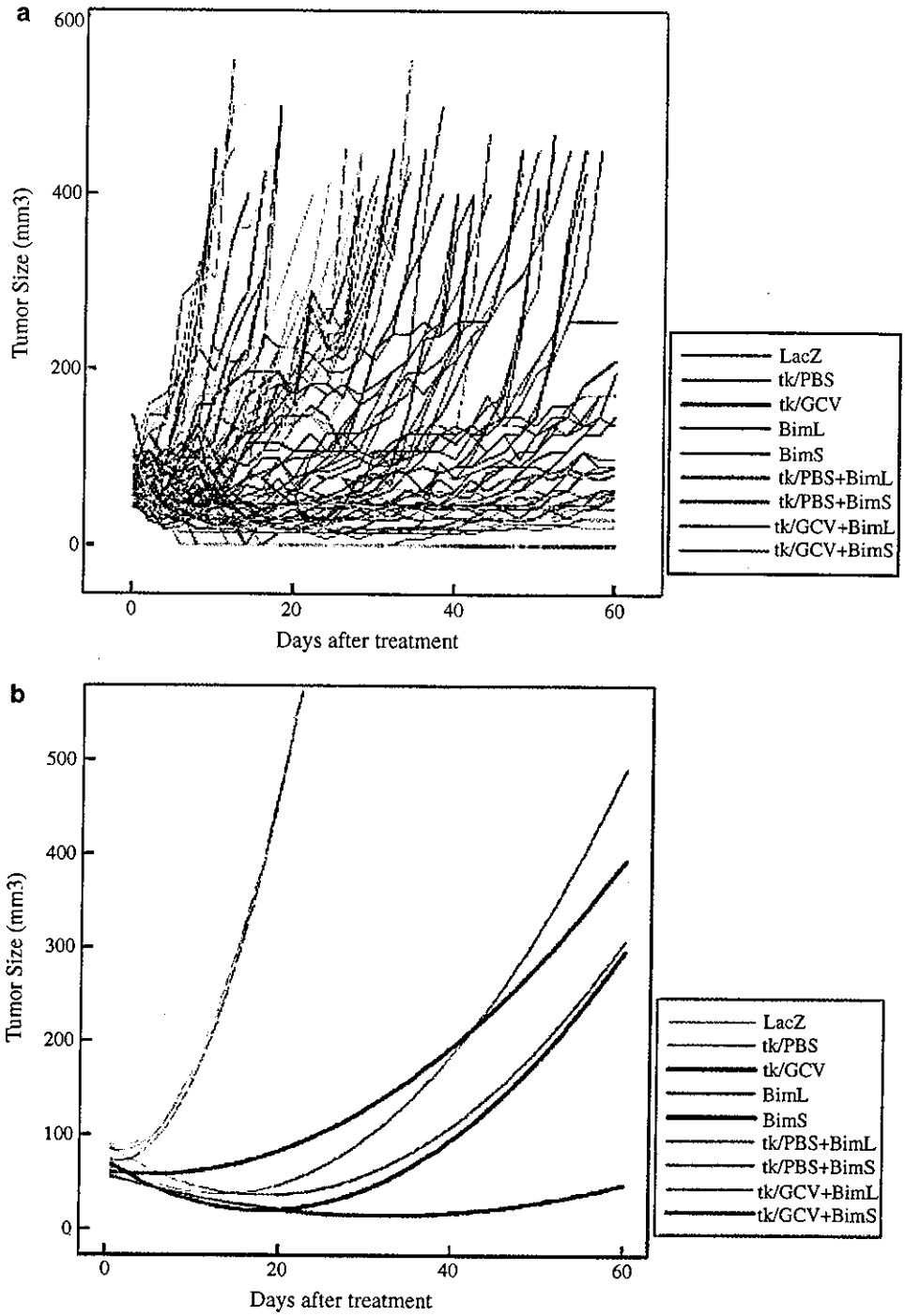

Figure 6 Effects of adenovirus infection on xenograft growth. U251 cells were inoculated subcutaneously into BALB/c nu/nu mice. Five days after the inoculation of cells, tumors that reached an average volume of 75 mm³ were subjected to intratumoral injection of adenovirus vectors indicated in insets. Animals inoculated with AVC2-tk were further injected i.p. with either GCV (tk/GCV) or PBS (tk/PBS) twice daily for 10 consecutive days. Tumor size was evaluated every 2 days until day 60 or till the tumor volume reached 400 mm³. The growth curve for each tumor treated by methods indicated in an inset (a), and the fitted growth curves for each treatment (b) were shown.

Materials and methods

Cell lines and cell culture

The cell lines established from human malignant gliomas that were used in this study were U251, U87MG (provided by RIKEN Cell Bank, Tsukuba, Japan), T-430 (a gift of Dr Kawamoto), U373 (a gift of Dr Kasahara), and A172 (provided by Tohoku University). A human leukemia cell line, HL-60 (provided by RIKEN Cell Bank), was used as a control for Bim expression. U251, U87, and A172 cells were cultured in Dulbecco's Modified Eagle Medium (D-MEM) supplemented with 10% fetal bovine serum (FBS); T-430, U373, and HL-60 cells were cultured in RPMI-1640 medium that was also supplemented with 10% FBS. 293B cells were established by transfecting human embryonic kidney 293 cells with

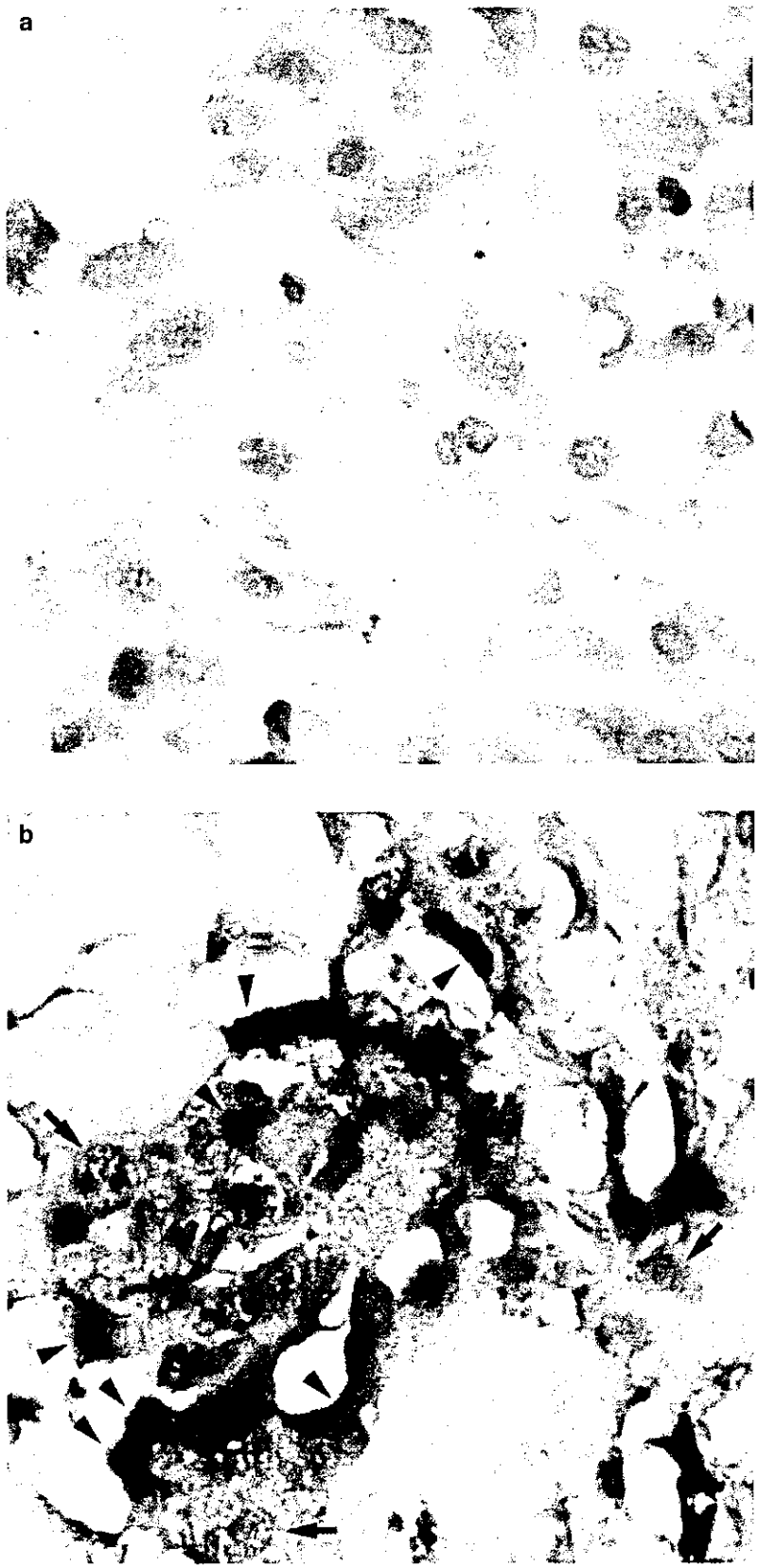

Figure 7 Expression of BimS in TUNEL-positive tumor cells in animal models. U251 cells inoculated subcutaneously into nude mice were subjected to TUNEL assay (black) and immunohistochemical analysis using an affinity-purified Bim antibody (red) before (a) and 3 days after infection by AVC2-BimS (b). Arrowheads indicate cells expressing Bim protein at high levels with TUNEL-positive nuclei. Arrows indicate cells expressing Bim protein at background levels with healthy nuclei. Sections were counterstained with methyl green.

pSFFV-neo-Bcl-x_L (a gift of Dr LH Boise) using the calcium phosphate method. Cells were cultured for 2 weeks in medium containing G418 (Gibco BRL, Rockville, MD, USA) at a concentration of 0.5 mg/ml. A clone with high expression of Bcl-x_L protein (293B) was isolated. 293 and 293B cells were cultured with D-MEM/F12 (1:1 mixture) supplemented with 10% FBS.

Construction and preparation of adenoviral vectors

The recombinant adenoviral vectors were constructed using an adenoviral DNA–protein complex lacking an insert (AVC2.null),[36] which contained the cytomegalovirus (CMV) promoter, a simian virus (SV)-40 intron, and the SV-40 polyadenylation signal. To generate AVC2-BimS or AVC2-BimL vectors encoding either BimS or BimL protein as well as the enhanced green fluorescence protein (EGFP) as a marker, a *Spe*I-*Cla*I fragment containing either *BimS* or *BimL* cDNA and an internal ribosomal entry site (IRES) sequence followed by the *EGFP* cDNA in frame was inserted into the *Xba*I and *Nsp*V sites in AVC2.null using the direct *in vitro* ligation technique.[36] To obtain AVC2-tk, the HSV-*tk* gene was excised from pAVS6TK[37] by digestion with *Xba*I and *Cla*I and ligated into AVC2.null. The adenovirus vector AVC2-LacZ harboring a β-galactosidase expression cassette has been previously described.[38] The ligated DNA–protein complex was introduced into 293 cells using the calcium phosphate transfection method. Viral isolates were screened and amplified using standard techniques.[36] Recombinant adenovirus was titered by determination of the median tissue culture infection dose ($TCID_{50}$). Viral stocks were stored in 10% glycerol and kept at −80°C until use.

Antibodies, immunoblot analysis

Anti-human Bcl-2 monoclonal antibody and anti-human Bcl-x polyclonal antibody were purchased from BD Transduction Laboratories (Lexington, KY, USA). Bax antibody was purchased from BD PharMingen (San Diego, CA, USA). Anti-Bim polyclonal antibody was raised by us and described elsewhere.[11] Affinity purification of the Bim antibody was performed using cyanogen bromide-activated Sepharose 4B (Amersham, Piscataway, NJ, USA) conjugated with antigen protein according to standard procedure. Immunoblot analysis was performed as described previously.[6,11] In each experiment, total cell extracts from 1×10^5 glioma cells or from 1×10^6 HL-60 cells were analyzed.

Terminal deoxynucleotidyltransferase-mediated nick end labeling (TUNEL) analysis

U251 cells were infected with AVC2-BimS or AVC2-BimL at an MOI of 20. Thirty-six hours later, cells were harvested and fixed with 4% paraformaldehyde for 20 min, and the TUNEL assay was performed using the Apoptosis Detection Kit according to the manufacturer's directions (Promega, Madison, WI, USA). Cells were then stained with 1 µg/ml propidium iodide (PI) and 0.1% Evans blue for 10 min at room temperature. After centrifugation with cytospin, incorporation of dUTP was visualized by fluorescence microscopy.

Microculture tetrazolium dye (XTT) assay

Cytotoxicity assays were performed using a vital stain XTT assay using the Cell Proliferation Kit II (Roche, Basel, Switzerland). U251 cells were seeded on 96-well plates and infected with AVC2-tk, AVC2-BimS, AVC2-BimL, or AVC2-tk in combination with AVC2-BimS or AVC2-BimL at a variety of MOIs. Forty-eight hours after AVC2-tk infection, either GCV at a final concentration of 10 µM or phosphate buffer saline (PBS) was added in the culture medium. Three or 7 days after infection, the tetrazolium salt 2,3-bis[2-methoxy-4-nitro-5-sulfophenyl]-2H-tetrazolium-5-carboxyaniline (XTT), which is metabolized to formazan by intact mitochondrial dehydrogenases, and an electron coupling reagent were added and cells were incubated for a further 24 hours. The viability of the cells was estimated on the basis of formazan formed, which was detected spectrophotometrically.

Adenovirus treatment in vivo

Athymic female BALB/c *nu/nu* mice purchased from Clea Japan (Tokyo, Japan) were inoculated subcutaneously (s.c.) with U251 cells (4×10^6 cells) in 100 µl Hank's balanced salt solution (HBSS) containing 50% (v/v) basement membrane matrix (Matrigel, BD Biosciences, Franklin Lakes, NJ, USA). Tumors were allowed to grow *in vivo* for 5 days, by which time they reached an average volume of 75 mm^3 (approximately 7.5×10^7 cells; tumor volumes were calculated as $a \times b^2 \times 0.5$, where a is the length and b is the width of the tumor in millimeters). Intratumoral injections of AVC2-BimS, AVC2-BimL, AVC2-tk, AVC2-LacZ (1.5×10^9 pfu/dose), and AVC2-tk in combination with AVC2-BimL or AVC2-BimS (0.75×10^9 pfu/dose, for each adenovirus) were then administered. Animals received AVC2-tk as a sole vector or those received AVC2-tk in combination with AVC2-BimL or AVC2-BimS were treated with an intraperitoneal (i.p.) injection of either GCV (50 mg/kg) in 1 ml PBS or PBS alone twice daily for 10 consecutive days. Ten mice were investigated in each group. Tumor size was measured every 2 days until day 60 or till the tumor volume reached 400 mm^3.

Immunohistochemical analysis

Subcutaneous tumors before and after infection by AVC2-BimS were harvested. Formalin-fixed and paraffin-embedded sections were incubated for 2 h with the affinity-purified Bim antibody followed by incubation for an additional 1 h with biotin-conjugated anti-rabbit IgG (Vector, Burlingame, CA, USA). The sections were incubated for 1 h with alkaline phosphatase streptavidin and then developed using Alkaline phosphatase substrate kit (Vector) according to the manufacturer's direction. TUNEL analysis was performed using Apoptosis *in situ* detection kit (Wako, Osaka, Japan) following the manufacturer's direction. Sections were counterstained with methyl green before mounting.

Acknowledgements

This work was supported in part by Grants-in-Aid for Scientific Research from the Ministry of Education, Culture, Sports, Science and Technology of Japan.

References

1 Moolten FL, Wells JM, Heyman RA, Evans RM. Lymphoma regression induced by gancyclovir in mice bearing a herpes thymidine kinase transgene. *Hum Gene Ther* 1990; **1**: 125–134.

2 Culver KW *et al*. *In vivo* gene transfer with retroviral vector-producer cells for treatment of experimental brain tumors. *Science* 1992; **256**: 1550–1552.

3 Bi WL, Parysek LM, Warnick R, Stambrook PJ. *In vitro* evidence that metabolic cooperation is responsible for the bystander effect observed with HSV tk retroviral gene therapy. *Hum Gene Ther* 1993; **4**: 725–731.

4 Ram Z *et al*. Therapy of malignant brain tumors by intratumoral implantation of retroviral vector-producing cells. *Nat Med* 1997; **3**: 1354–1361.

5 Rainov NG. A phase III clinical evaluation of herpes simplex virus type 1 thymidine kinase and ganciclovir gene therapy as an adjuvant to surgical resection and radiation in adults with previously untreated glioblastoma multiforme. *Hum Gene Ther* 2000; **11**: 2389–2401.

6 Kuribara R *et al*. Two distinct interleukin-3-mediated signal pathways, Ras-NFIL3(E4BP4) and Bcl-x_L, regulate the survival of murine pro-B lymphocytes. *Mol Cell Biol* 1999; **19**: 2754–2762.

7 Packham G *et al*. Selective regulation of Bcl-XL by a Jak kinase-dependent pathway is bypassed in murine hematopoietic malignancies. *Genes Dev* 1998; **12**: 2475–2487.

8 Dumon S *et al*. IL-3 dependent regulation of Bcl-x_L gene expression by STAT5 in a bone marrow derived cell line. *Oncogene* 1999; **18**: 4191–4199.

9 Silva M *et al*. Erythropoietin can induce the expression of bcl-x(L) through Stat5 in erythropoietin-dependent progenitor cell lines. *J Biol Chem* 1999; **274**: 22 165–22 169.

10 Socolovsky M *et al*. Fetal anemia and apoptosis of red cell progenitors in Stat5a-/-5b-/- mice: a direct role for Stat5 in Bcl-X(L) induction. *Cell* 1999; **98**: 181–191.

11 Shinjyo T *et al*. Downregulation of Bim, a proapoptotic relative of Bcl-2, is a pivotal step in cytokine-initiated survival signaling in murine hematopoietic progenitors. *Mol Cell Biol* 2001; **21**: 854–864.

12 Kitada S *et al*. ;-Radiation induces upregulation of Bax protein and apoptosis in radiosensitive cells *in vivo*. *Oncogene* 1996; **12**: 187–192.

13 Toms S *et al*. Antagonist effect of insulin-like growth factor I on protein kinase inhibitor-mediated apoptosis in human glioblastoma cells in association with bcl-2 and bcl-xL. *J Neurosurg* 1998; **88**: 884–889.

14 Shu HK *et al*. The intrinsic radioresistance of glioblastoma-derived cell lines is associated with a failure of p53 to induce p21(BAX) expression. *Proc Natl Acad Sci USA* 1998; **95**: 14 453–14 458.

15 Craperi D *et al*. Increased bax expression is associated with cell death induced by ganciclovir in a herpes thymidine kinase gene-expressing glioma cell line. *Hum Gene Ther* 1999; **10**: 679–688.

16 Tsujimoto Y, Shimizu S. Bcl-2 family: life-or-death switch. *FEBS Lett* 2000; **466**: 6–10.

17 Dijkers PF *et al*. Expression of the pro-apoptotic Bcl-2 family member Bim is regulated by the forkhead transcription factor FKHR-L1. *Curr Biol* 2000; **10**:1201–1204.

18 Whitfield J *et al*. Dominant-negative c-Jun promotes neuronal survival by reducing BIM expression and inhibiting mitochondrial cytochrome c release. *Neuron* 2001; **29**: 629–643.

19 Putcha GV *et al*. Induction of BIM, a proapoptotic BH3-only BCL-2 family member, is critical for neuronal apoptosis. *Neuron* 2001; **29**: 615–628.

20 O'Connor L *et al*. Bim: a novel member of the Bcl-2 family that promotes apoptosis. *EMBO J* 1998; **17**: 384–395.

21 Hsu SY, Lin P, Hsueh AJ. BOD (Bcl-2-related ovarian death gene) is an ovarian BH3 domain-containing proapoptotic Bcl-2 protein capable of dimerization with diverse antiapoptotic Bcl-2 members. *Mol Endocrinol* 1998; **12**: 1432–1440.

22 King SM *et al*. Brain cytoplasmic and flagellar outer arm dyneins share a highly conserved Mr 8000 light chain. *J Biol Chem* 1996; **271**: 19 358–19 366.

23 Jaffrey SR, Snyder SH. PIN: an associated protein inhibitor of neuronal nitric oxide synthase. *Science* 1996; **274**: 774–777.

24 Puthalakath H *et al*. The proapoptotic activity of the Bcl-2 family member Bim is regulated by interaction with the dynein motor complex. *Mol Cell* 1999; **3**: 287–296.

25 Potthoff RF, Roy SN. A generalized multivariate analysis of variance model useful especially for growth curve problems. *Biometrika* 1964; **51**: 313–326.

26 Vonesh EF, Carter RL. Efficient inference for random-coefficient growth curve models with unbalanced data. *Biometrics* 1987; **43**: 617–628.

27 Adams JM, Cory S. The Bcl-2 protein family: arbiters of cell survival. *Science* 1998; **281**: 1322–1326.

28 de la Taille A *et al*. Apoptotic conversion: evidence for exchange of genetic information between prostate cancer cells mediated by apoptosis. *Cancer Res* 1999; **59**: 5461–5463.

29 Fadok VA, Henson PM. Apoptosis: getting rid of the bodies. *Curr Biol* 1998; **8**: R693-R695.

30 Mi J *et al*. Induced apoptosis supports spread of adenovirus vectors in tumors. *Hum Gene Ther* 2001; **12**: 1343–1352.

31 Karamitopoulou E, Perentes E, Diamantis I, Maraziotis T. Ki-67 immunoreactivity in human central nervous system tumors: a study with MIB 1 monoclonal antibody on archival material. *Acta Neuropathol* (Berl) 1994; 87: 47–54.

32 Brenner M *et al*. GFAP promoter directs astrocyte-specific expression in transgenic mice. *J Neurosci* 1994; **14**: 1030–1037.

33 Miura M, Tamura T, Mikoshiba K. Cell-specific expression of the mouse glial fibrillary acidic protein gene: identification of the cis- and trans-acting promoter elements for astrocyte-specific expression. *J Neurochem* 1990; 55: 1180–1188.

34 Miura M, Tamura T, Aoyama A, Mikoshiba K. The promoter elements of the mouse myelin basic protein gene function efficiently in NG108-15 neuronal/glial cells. *Gene* 1989; **75**: 31–38.

35 Miyao Y *et al*. Selective expression of foreign genes in glioma cells: use of the mouse myelin basic protein gene promoter to direct toxic gene expression. *J Neurosci Res* 1993; **36**: 472–479.

36 Okada T *et al*. Efficient directional cloning of recombinant adenovirus vectors using DNA–protein complex. *Nucleic Acids Res* 1998; **26**: 1947–1950.

37 Okada T *et al*. AV.TK-mediated killing of subcutaneous tumors *in situ* results in effective immunization against established secondary intracranial tumor deposits. *Gene Ther* 2001; **8**: 1315–1322.

38 Leimig T *et al*. High-efficiency transduction of freshly isolated human tumor cells using adenoviral interleukin-2 vectors. *Hum Gene Ther* 1996; **7**: 1233–1239.

Available online at www.sciencedirect.com
SCIENCE DIRECT®
Neuroscience Research 45 (2003) 33–40
Neuroscience Research
www.elsevier.com/locate/neures

Intramuscular injection of AAV-GDNF results in sustained expression of transgenic GDNF, and its delivery to spinal motoneurons by retrograde transport

Yan-Yan Lu[a,b,1], Li-Jun Wang[a,b], Shin-ichi Muramatsu[a,*], Kunihiko Ikeguchi[a], Ken-ichi Fujimoto[a], Takashi Okada[b], Hiroaki Mizukami[b], Takashi Matsushita[b], Yutaka Hanazono[b], Akihiro Kume[b], Toshiharu Nagatsu[c], Keiya Ozawa[b], Imaharu Nakano[a,*]

[a] *Division of Neurology, Department of Medicine, Jichi Medical School, 3311-1 Yakushiji, Minamikawachi-machi, Tochigi 329-0498, Japan*
[b] *Division of Genetic Therapeutics, Center for Molecular Medicine, Jichi Medical School, 3311-1 Yakushiji, Minamikawachi-machi, Tochigi 329-0498, Japan*
[c] *Institute for Comprehensive Medical Science, Fujita Health University, Toyoake, Aichi 470-1192, Japan*

Received 11 July 2002; accepted 13 September 2002

Abstract

Adeno-associated virus (AAV) vector has been developed as an attractive gene delivery system with proven safety. Glial cell line-derived neurotrophic factor (GDNF) is proposed to be a promising therapeutic agent for amyotrophic lateral sclerosis (ALS) and other motor neuron diseases. The purpose of this report was to investigate transgenic GDNF expression at different time points post AAV mediated GDNF intramuscular delivery. An AAV vector was constructed to encode a recombinant fusion of GDNF tagged with a FLAG sequence at the C-terminal (AAV-GDNF) to distinguish it from its endogenous counterpart. A single intramuscular injection of AAV-GDNF led to substantial expression of transgenic GDNF which remained for at least 10 months in transduced gastrocnemius muscle. This transgenic GDNF was distributed in a large number of myofibers, mainly in the vicinity of the sarcolemma and predominantly concentrated at the sites of neuromuscular junctions (NMJs). Furthermore, transgenic GDNF, but not β-galactosidase expressed as a control, was detected in the motoneurons that projected axons to the injected muscles, thus, indicating retrograde axonal transportation of the transgenic GDNF. This study provides a basis for a strategy of intramuscular AAV-GDNF delivery to protect motoneurons as a possible means of ALS treatment.

Keywords: Adeno-associated virus (AAV); Glial cell line-derived neurotrophic factor (GDNF); Gene therapy; Motoneurons; Intramuscular injection; Retrograde transport

1. Introduction

Glial cell line-derived neurotrophic factor (GDNF) has been demonstrated to be the most potent neurotrophic factor yet described for motoneurons, and was proposed to be a promising therapeutic agent for motor neuron diseases like amyotrophic lateral sclerosis (ALS), as supported by in vivo and in vitro results (Henderson et al., 1994; Oppenheim et al., 1995; Yan et al., 1995). So far, however, clinical trials with GDNF or the other neurotrophic factors, such as ciliary neurotrophic factor (CNTF), brain-derived neurotrophic factor (BDNF), or insulin-like growth factor I (IGF-I), with repeated administration as the recombinant protein, have revealed severe side effects and/or limited (or even no) clinical benefits (Yuen, 2001). The reasons for this failure include the short in vivo half-life of the recombinant protein, poor access to spinal motoneurons and inflammatory effects etc. These limitations, together

* Corresponding authors. Tel.: +81-285-58-7351; fax: +81-285-44-5118 (I.N.); tel.: +81-285-58-7352; fax: +81-285-44-5118 (S.M.)
E-mail addresses: muramats@ms.jichi.ac.jp (S.-i. Muramatsu), inakano@ms.jichi.ac.jp (I. Nakano).
[1] Stem Cell Research Center, Health Science Center, Peking University, Beijing 100083, People's Republic of China.

0168-0102/02/$ - see front matter
PII: S0168-0102(02)00195-5

with the chronicity of motor neuron diseases, underscore the necessity to develop innovative strategies for more effective delivery of neurotrophic factors to motoneurons. Vector-mediated gene delivery may resolve this problem well, in a manner whereby the factor is continuously synthesized in the desired tissue (Alisky and Davidson, 2000).

Among the transgene delivery systems now available, adeno-associated virus (AAV) vectors have drawn considerable interest by virtue of their unparalleled merits. As the only viral vector system based on a nonpathogenic and replication-defective virus, an AAV vector has been successfully used for efficient and sustained gene transfer to both proliferating and terminally differentiated cells in a variety of tissues without a detectable immune response or toxicity (Bueler, 1999). Previous experiments have demonstrated that AAV is effective for long-term delivery of GDNF at biologically relevant levels in the nigrostriatal system (Mandel et al., 1999; Kirik et al., 2000; Wang et al., 2002a). The neuroprotective effects of transgenic GDNF on dopaminergic neurons, by means of its retrograde transport from dendrites in the striatum to neuron bodies in the substantia nigra, imply the potential to employ a similar strategy for ALS gene therapy. Indeed, an intramuscular injection of an AAV encoding GDNF has been successfully employed to increase the survival of motoneurons and prolong the life span in transgenic ALS mice (Wang et al., 2002b). However, this report doesn't reveal transgenic GDNF levels at different time points after the intramuscular AAV vector injection. Aimed at choosing more suitable windows for ALS treatment, the purpose of this study was to determine transgenic GDNF levels at different time points post a single AAV-GDNF intramuscular injection, and its retrograde transport to spinal motoneurons.

2. Materials and methods

2.1. AAV vector production

The construction and production of AAV type 2 vector encoding a recombinant GDNF protein fusion tagged with a FLAG peptide (AAV-GDNF) were as previously described (Wang et al., 2002a). The recombinant mouse GDNF was tagged with a FLAG sequence (DYKDDDDK) at the carboxyl terminus to distinguish it from its endogenous counterpart. AAV vectors were produced in an adenovirus-free system by means of the three plasmids co-transfection method and then purified with two sequential continuous CsCl gradients (Matsushita et al., 1998). The final particle titers were 1.6×10^{13} vector genome copies per ml for the AAV-GDNF vector and 2.1×10^{13} vector genome copies per ml for the AAV-LacZ vector, as determined by quantitative DNA dot-blot hybridization analysis.

2.2. In vitro expression of GDNF

Human embryonic kidney 293 (HEK293) cells (2×10^5) were seeded onto 35 mm-diameter dishes and then allowed to proliferate overnight in Dulbecco's modified Eagle's medium (DMEM, Gibco BRL) supplemented with 10% heat inactivated fetal bovine serum (FBS). When cells reached approximately 80% confluence, they were infected for 5 h with AAV-LacZ or AAV-GDNF vector at the indicated genome copies in DMEM supplemented with 2% FBS. Then, the culture medium (CM) was refreshed with DMEM without FBS. After 48 h incubation, the supernatant was collected as CM. GDNF levels in both the CM and the cell lysates were examined by ELISA.

2.3. In vivo administration of AAV vectors

C57BL/6J mice (7 weeks old) were injected with either the AAV-GDNF ($n = 32$) or AAV-LacZ ($n = 21$) vector into the left gastrocnemius muscle using a microsyringe connected to a 27-gauge needle. A total of 2×10^{10} AAV genome copies in 24 μl PBS were injected into each muscle at three sites. As a sham control, the right gastrocnemius muscle was injected with the same volume of PBS. No morbidity or mortality was observed in the mice during the experimental period.

The biological activity of transgenic GDNF in vitro has been demonstrated in our previous study (Wang et al., 2002a), all mice were handled according to approved animal protocols in Jichi Medical School (Japan).

2.4. Tissue preparations

At the indicated time, gastrocnemius muscles were dissected out, rapidly frozen in liquid nitrogen-cooled isopentane, and stored at −80 °C for ELISA analysis or cryostat sectioning. The mice were then perfused with ice-cold PBS followed by 4% paraformaldehyde (PFA). The spinal cord was dissected out, post-fixed for 4 h in 4% PFA, and then cryoprotected by soaking sequentially in 10, 20 and 30% sucrose at 4 °C overnight. Serial transverse cryostat sections of frozen muscle tissue (10 μm) were thawed, mounted on slides coated with gelatin, and then completely dried before storing at −80 °C. Serial transverse sections of the lumbar spinal cord (30 μm thickness) were cut with a freezing microtome and stored in PBS at 4 °C.

2.5. GDNF ELISA

The GDNF levels in CM, HEK293 cell and gastrocnemius muscle lysates were determined by ELISA

(GDNF E_{max} ImmunoAssay System, Promega). For detection in cell and gastrocnemius muscle lysates, cells or tissues were homogenized in lysis buffer (137×10^{-3} mol/l NaCl, 20×10^{-3} mol/l Tris [pH 8.0], 1% NP40, and 10% glycerol, supplemented with Protease Inhibitor Cocktail Tablets Complete Mini [Roche]), ultrasonicated, and then centrifuged at 4 °C. The supernatants were acidified and then neutralized to pH 7.4 before assaying. Acidification has been reported to enhance the detection of neurotrophic factors (Okragly and Haak-frendscho, 1997). Triplicate samples were processed in 96-well plates according to the protocol recommended by the manufacturer. Briefly, plates were coated with anti-GDNF monoclonal antibodies, blocked, and then incubated with GDNF standards or samples. The plates were then incubated sequentially with chicken anti-human GDNF polyclonal antibodies and anti-chicken IgY-peroxidase conjugate, followed by a peroxidase substrate and tetramethylbenzidine solution for color development. The reaction was stopped with 1 N hydrochloric acid and the absorbance at 450 nm was read. GDNF levels were expressed as ng per (10^5 cells, 24 h) for cell cultures and pg/mg tissue for gastrocnemius muscles. The assay sensitivity ranged from 16 to 1000 pg/ml.

2.6. β-Galactosidase histochemistry

For β-galactosidase (β-Gal) histochemistry, muscle sections were fixed and stained for 4–6 h with a 5-bromo-4-chloro-3-indolyl-β-D-galactopyranoside (X-Gal) staining solution (500 μg/ml X-Gal, 5 mM potassium ferricyanide, 5 mM potassium ferrocyanide, 0.01% sodium deoxycholate, 0.02% Nonidet P-40, and 2 mM magnesium chloride in PBS) at 37 °C. Spinal cord samples were stained as free-floating sections and mounted on gelatin-coated slides to allow them to dry. Sections were counterstained with eosin for detection.

2.7. Immunohistochemistry

Immunohistochemistry staining with anti-FLAG antibodies was performed on cryostat sections of gastrocnemius muscle to detect transgenic GDNF and to distinguish it from endogenous GDNF. Sections were fixed with cool acetone, treated with 0.3% H_2O_2, sequentially incubated with an anti-FLAG antibody (1:1000, rabbit polyclonal anti-FLAG antibody; Sigma) overnight at 4 °C, a biotinylated secondary antibody to rabbit IgG (1:400) for 2 h, and then visualized by the avidin-biotinylated peroxidase complex procedure (Vectastain ABC kit; Vector Laboratories Inc., Burlingame, CA), using 3,3-diaminobenzidine (DAB) as a chromogen. For double immunofluorescence staining, muscle sections were stained with a Mouse-on-Mouse kit (M.O.M™ kit; Vector Laboratories Inc., Burlingame, CA) according to the manufacturer's protocol. The primary antibodies used for muscle sections were mouse anti-FLAG M2 (1:500; Sigma) and rabbit anti-GDNF (1:1000; Santa Cruz) ones. After incubation of the primary antibodies at 4 °C overnight, the sections were incubated with corresponding rhodamine or FITC-conjugated secondary antibodies for detection. For double immunofluorescence staining of FLAG and α-bungarotoxin, sections were incubated with the rabbit anti-FLAG antibody first, followed by incubation with the FITC-conjugated anti-rabbit secondary antibody and a tetramethly-rhodamine conjugated α-bungarotoxin molecular probe (1:400; Molecular Probes Inc., Eugene, USA). α-Bungarotoxin is a peptide that specifically binds with high affinity to the α-subunit of the acetylcholine receptor (AchR) on the postsynaptic membrane of neuromuscular junctions (NMJs). To trace the transgenic GDNF in the spinal cord, primary antibodies used were rabbit anti-FLAG (1:1000; Sigma) and mouse anti-NeuN (1:200; Chemicon) ones. Sections were then incubated with corresponding rhodamine or FITC-conjugated secondary antibodies for detection. Immunofluorescently stained sections were viewed and photographed under a confocal laser scanning microscope (TCS NT; Leica, Heidelberg, Germany).

3. Results

3.1. In vitro expression of GDNF

HEK293 cells were infected with the AAV-GDNF or AAV-LacZ vector in the range of $0.5–18 \times 10^3$ vector genomes per cell. ELISA analysis revealed high levels of GDNF expression and secretion in AAV-GDNF transduced cells (Fig. 1). As expected, the GDNF level in the CM was much higher than that in the cell lysates, indicating that GDNF was mainly secreted by transduced cells. Moreover, in the genome copy range used, the amounts of GDNF in CM and cell lysates showed genome copy-dependent increases. In non-transduced or AAV-LacZ transduced HEK293 cells, the GDNF level was much lower, being barely above the detection limit of the ELISA analysis.

3.2. In vivo expression of GDNF in AAV vector-injected gastrocnemius muscles of mice

ELISA determination of the GDNF levels in AAV-GDNF injected gastrocnemius muscles showed that GDNF expression could be detected at 14 days post-injection, gradually increased in the first 2 months, and then remained constant without significant diminution until 6 months (Fig. 2). Although there was a slight reduction from 8 months postinjection, substantial expression persisted until at least 10 months postinjec-

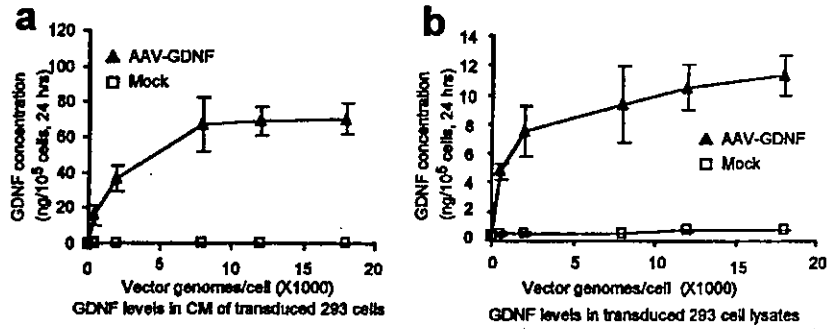

Fig. 1. CM, (a) and cell lysates (b) were collected 48 h post-infection with the AAV-GDNF or AAV-LacZ vector, and then the GDNF levels were determined by ELISA analysis. The CM and cell lysates both exhibited a dose-dependent increase in GDNF. Compared with those in CM, the GDNF levels in cell lysates were relatively low, consistent with the secretory property of GDNF. In both CM and cell lysates, the GDNF levels in untransduced or AAV-LacZ vector-transduced cells were much lower, i.e. barely above the detection limit of the ELISA. The results are presented as the averages of triplicate determinations.

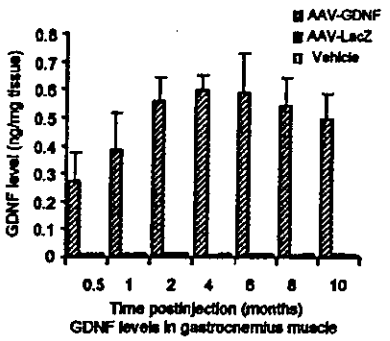

Fig. 2. GDNF levels in gastrocnemius muscle after intramuscular AAV vector injection, as detected by ELISA. Data represent means ± S.E. (AAV-GDNF, $n = 4$; AAV-LacZ, $n = 3$; PBS, $n = 4$).

tion, the longest time we observed till now. The gastrocnemius muscles injected with the AAV-LacZ vector or PBS exhibited very low levels of GDNF.

3.3. Distribution pattern of the transgene-derived GDNF in gastrocnemius muscles

In gastrocnemius muscles injected with AAV-GDNF, substantial and sustained immunoreactive signals for FLAG were detected in a large number of myofibers from 2 weeks to 10 months postinjection (Fig. 3b and c). FLAG immunoreactive myofibers were stably ranging from 28 to 35% of the muscle cross-section over 6 months, with slight decrease to about 20% at 10 months. Double-immunofluorescence staining with anti-GDNF and anti-FLAG antibodies showed co-localization of GDNF and FLAG immunoreactivity (Fig. 3d–f), confirming the existence of a GDNF-FLAG fusion protein. Intense immunoreactivity was concentrated in the vicinity of the sarcolemma, suggesting effective secretion of transgenic GDNF by myofibers. In AAV-LacZ or PBS-injected muscles, only weak immunosignals for GDNF, but not for FLAG, were detected in the vicinity of the sarcolemma (data not shown). This is in agreement with the ELISA results, indicating that the GDNF detected on ELISA in AAV-LacZ or PBS-injected muscles is endogenous GDNF.

To determine whether or not the neurotrophic theory for GDNF also applies to transgenic GDNF, double-immunofluorescence staining with anti-FLAG antibodies and rhodamine-conjugated α-bungarotoxin was performed on gastrocnemius muscle sections. Confocal microscopy revealed colocalization of more intense immunoreactivity of FLAG with signals of α-bungarotoxin, indicating the concentration of the transgenic GDNF in the vicinity of NMJs (Fig. 3g–i). In AAV-LacZ or PBS-injected muscles, only α-bungarotoxin signals indicating NMJs could be detected.

In the gastrocnemius muscles injected with AAV-LacZ, β-Gal activity was detected in a large number of myofibers (Fig. 3a). The signals were distributed evenly within the sarcoplasms, an expression pattern totally different from that of transgenic GDNF. Sustained expression was detected from 2 weeks to at least 10 months postinjection, with a trend of slight diminution from 8 months postinjection.

These results showed that a single injection of AAV-GDNF into the gastrocnemius muscle allowed durable and substantial expression of transgenic GDNF, which was mainly in the vicinity of the sarcolemma and predominantly accumulated at the NMJs, implying a possible uptake of transgenic GDNF by nerve terminals at NMJs.

3.4. Retrograde transport of transgene-derived GDNF to spinal motoneurons

We further examined whether or not transgenic GDNF could also be retrogradely transported from muscle to spinal motoneurons through a similar mechanism as previously reported for GDNF delivered as a protein (Leitner et al., 1999). Double-immunostaining

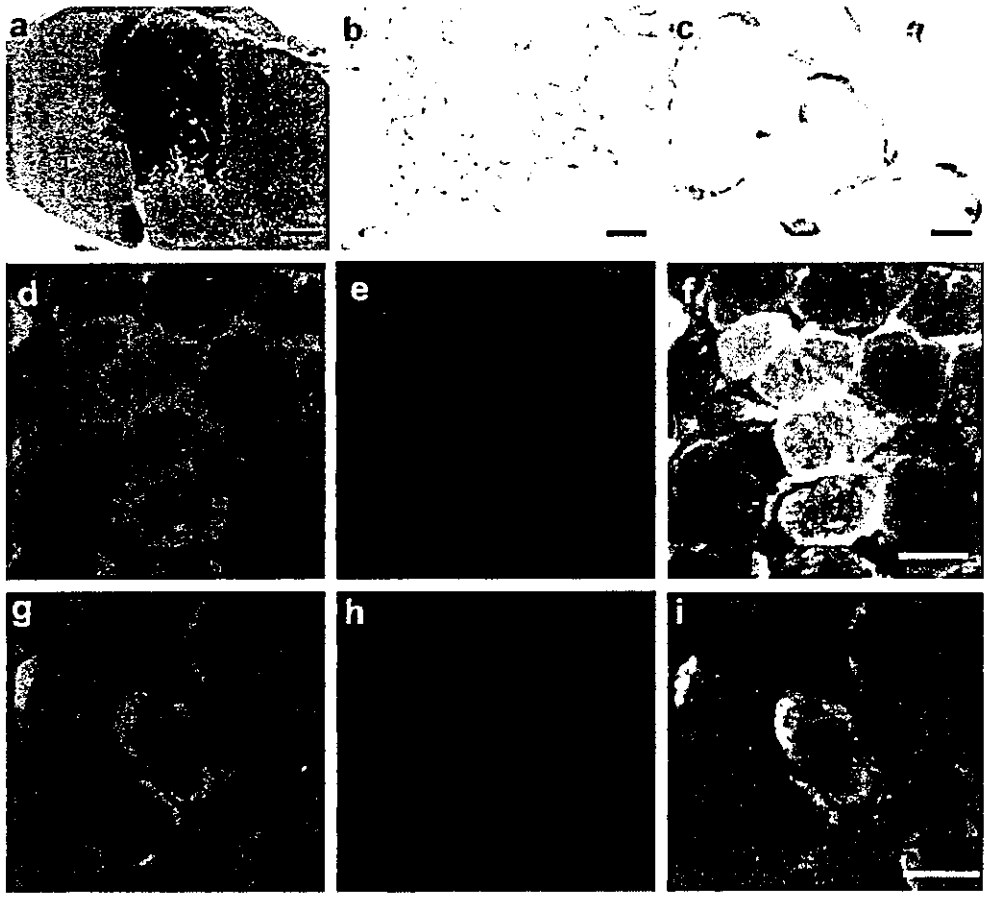

Fig. 3. Representative photographs of AAV vector-mediated transgene expression in gastrocnemius muscles 4 months after AAV-GDNF vector injection. (a) β-Galactosidase signals in AAV-LacZ vector-injected muscle. In AAV-GDNF-*FLAG* vector-injected muscle, FLAG immunoreactivity was widely distributed in myofibers (b low magnification), intense immunoreactivity being observed mainly in the vicinity of the sarcolemma (c high magnification). Double-immunofluorescence staining with anti-FLAG (d) and anti-GDNF (e) antibodies demonstrated co-localization of GDNF and FLAG signals [(f), merging of (d) and (e)]. More intense immunoreactivity for FLAG (g) was localized in postsynaptic AchR-rich regions revealed by α-bungarotoxin (h), indicating the accumulation of the transgenic GDNF fusion protein at NMJs [(i), merging of (g) and (h)]. Scale bars: (a) 800 μm; (b) 100 μm and (c) 25 μm. Scale bar in (f): (d–f) 50 μm. Scale bar in (i): (g–i) 50 μm.

with anti-FLAG and anti-NeuN (a specific marker of neurons) antibodies was performed on spinal cord sections (lumbar four to six) corresponding with the innervation of gastrocnemius muscles. FLAG immunoreactivity was detected in NeuN-positive cells of the ventral horn ipsilateral to the AAV-GDNF injected side. The large size (diameter > 20 μm), ventral horn distribution and NeuN-positive characteristics of these FLAG-immunoreactive cells were supposed to be α-motoneurons (Fig. 4). As anti-FLAG antibodies ex-

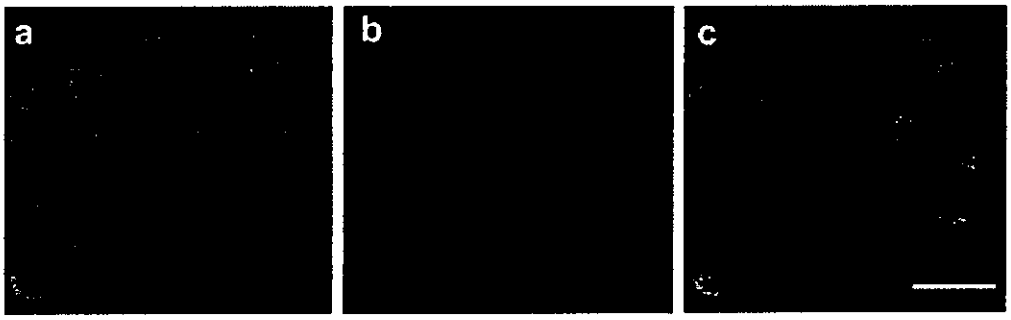

Fig. 4. Transgenic GDNF in spinal motor neurons, as detected with anti-FLAG antibodies, 4 weeks after AAV-GDNF vector injection. Merging (c) of the FLAG (a) and NeuN (b) signals shows their co-localization in the motoneurons of the spinal cord ventral horn. Scale bar, 50 μm.

cluded the interference of endogenous GDNF, this suggested the existence of the transgenic GDNF in the motoneurons. At 4 weeks postinjection, FLAG-positive neurons dispersed in the ventral horns reached about 6% of the total NeuN-positive neurons spanning lumbar four to six. Similar ratio of FLAG-positive neurons persisted without significant decrease over 6 months, indicating stable access of transgenic GDNF to spinal motoneurons. From 8 to 10 months postinjection, FLAG signals were relatively hard to detect in the corresponding spinal motoneurons. As expected, no FLAG signal was detected in the contralateral ventral horn of the same section and in the ventral horns of either AAV-LacZ or PBS-injected mice.

In order to determine whether or not AAV vector itself could be retrogradely transported, X-Gal staining was performed on the corresponding spinal cord sections in AAV-LacZ injected mice at different time points (1, 2, 4, 6, 8 and 10 months postinjection). We could not trace β-Gal signals in the corresponding ventral horns at any time point, in spite of the wide distribution of β-Gal signals in the muscles.

4. Discussion

We reported in this study that a single intramuscular injection of AAV-GDNF led to substantial and long-lasting transgenic GDNF expression in transduced muscles in mice, as detected by immunohistochemistry and ELISA. Considering the wide distribution of endogenous GDNF in the muscles and its up-regulation on the denervation (Yamamoto et al., 1999), it is necessary to distinguish transgenic GDNF from its endogenous counterpart while evaluating gene delivery efficiency. In this report, we solved this problem by adding a FLAG tag to transgenic GDNF, confirming that it was the transgenic GDNF that was greatly expressed at as high as nanogram level in the treated muscles.

With the substantial amount of transgenic GDNF sustained for as long as 10 months in gastrocnemius muscles of mice, a slight decrease was observed from 8 months post-injection. This is consistent with reports by other groups as well as ours for the striatum (Verma and Somia, 1997; Wang et al., 2002a). In spite of several hypotheses regarding the mechanism underlying this decrease in transgene expression, the actual mechanism remains to be clarified (Verma and Somia, 1997; Rabinowitz and Samulski, 1998). Additionally, anti-AAV neutralizing antibodies were reported in the serum after its intramuscular injection in mice and non-human primates (Chirumle et al., 2000). Despite such an unsolved problem and disadvantageous situation, the feasibility of repeated AAV vector re-administration has been successfully demonstrated (Chirumle et al., 2000), giving rise to the possibility of longer term expression of a transgene.

Transgenic GDNF distribution detected with anti-FLAG antibodies in this report is similar to that of endogenous GDNF observed in healthy human (Suzuki et al., 1998), as well as in ALS mouse muscles transduced with AAV-GDNF (Wang et al., 2002b). According to the neurotrophic theory, a neurotrophic factor is synthesized and released by the targets of neurotrophic factor-dependent axons, where it is bound and uptaken by receptors on axon terminals, and then retrogradely transported to the neuronal bodies (Distefano, 1993). Receptor-mediated retrograde transport of exogenous GDNF protein has been reported in motoneurons of rats (Leitner et al., 1999). Although the physiological significance of the retrograde transport is not completely known, it is thought to be of critical importance in axon-target communication, the conveyance of a signal transduction complex and neuronal viability (Neet and Capenot, 2001). The accumulation of transgenic GDNF at NMJs suggests that, consistent with the neurotrophic theory, an NMJ is the site for the uptake of transgenic GDNF by nerve terminals as a target-derived neurotrophic factor.

We detected transgenic GDNF in spinal motoneurons of the ventral horn ipsilateral to the AAV-GDNF injected side. Here the transgenic GDNF might have been derived through three possible ways: systemic delivery, retrograde transport of AAV vectors, or the fusion protein itself. The restricted distribution and ipsilateral presentation in motoneurons, as well as the known inability of GDNF to pass through the blood-brain barrier, exclude the possibility of systematic delivery of transgenic GDNF to the spinal motoneurons. Retrograde transport of an AAV vector itself in the CNS was reported recently, using a reporter green fluorescent protein (GFP) as a tracer (Kaspar et al., 2002). However, because intramuscularly expressed β-Gal can not be secreted as itself out of muscle fibers to be transported through axons, our failure to detect its signal in spinal motoneurons of AAV-LacZ injected mice indicates that no or very little, if any, AAV vector particles were retrogradely transported. We, thus, assumed that the transgenic GDNF detected in the motoneurons was mainly derived through retrograde axonal transport of the GDNF protein, and not AAV-GDNF vectors. This is consistent with a previous report (Kordower et al., 2000) and our recently published data for the nigrostriatal system (Wang et al., 2002a), which also showed that it is difficult for an AAV vector per se to be retrogradely transported. The population of FLAG-positive motoneurons seemed low in the spinal cord, indicating that not all the corresponding motoneurons could gain access to transgenic GDNF through axonal retrograde transport. Since transduced muscle fibers provide long-term and efficient transgenic GDNF

delivery, the continuous retrograde transport of transgenic GDNF should be of great potent to the motoneurons. Additionally, to expect more motoneurons gaining access to transgenic GDNF, it is reasonable to choose more corresponding muscles for injection. In deed, multi-sites injection of AAV-GDNF into four limbs did result in substantial GDNF expression in transduced muscles, protecting spinal motoneurons and significantly prolonging the survival in transgenic ALS mice (Wang et al., 2002b).

GDNF exerts its effects through a multireceptor complex composed of a glycosylphosphatidylinositol-linked (GPI) GDNF receptor (GFRα-1) and a signaling component (Ret receptor tyrosine kinase; Jing et al., 1996). The target-derived mechanism of the GDNF action has been confirmed in the nigrostriatal system (Tomac et al., 1995). In the spinal cord, GFRα-1 and Ret are expressed prominently in motoneurons of the ventral horn (Leitner et al., 1999), which can still persist in the degenerating motoneurons of ALS cases (Mitsuma et al., 1999). Based on these previous results, our observation of retrograde transport of the transgenic GDNF to the motoneurons implies the potential of this strategy for ALS gene therapy through a similar mechanism. It is reported that transgenic overexpression of GDNF could lead to dramatic increase in the number of motor axons innervating muscle fibers at the NMJ (Nguyen et al., 1998). Subcutaneous injection of exogenous GDNF in postnatal mice increased the number of axons converging at NJMs and induced a state of continuous synaptic remodeling (Keller-Peck et al., 2001). We, thus, assumed that transgenic GDNF locally expressed in the muscles might also provide therapeutic benefit on ALS by promoting muscle viability and improving synaptic activity.

The sustained substantial expression of transgenic GDNF after a single intramuscular AAV-GDNF injection well meets the long-term demand of motoneurons for GDNF availability. The simplicity and manipulability of intramuscular injection keeps the regions of target neurons intact by preventing physical trauma. Thus, this strategy should be of first priority for ALS treatment. As the transgenic GDNF expression was detectable at 14 days postinjection and increased in the first 2 months, for ALS treatment, AAV-GDNF injection should be performed earlier to obtain enough transgenic GDNF in the transduced muscles, as well as in the corresponding motoneurons.

Acknowledgements

We thank Yaeko Nagatsuka and Yoshie Sato for their excellent technical assistance. We also thank Avigen Inc. for providing the AAV vector production system. This study was supported in part by a Grant-in-Aid for Scientific Research on Priority Areas and Special Coordination Funds for Promoting Science and Technology from the Ministry of Education, Culture, Sports, Science and Technology, The Japanese Government; by Health Sciences Research Grants from the Ministry of Health Labor and Welfare of Japan; by Core Research for Evolutional Science and Technology (CREST) of the Japan Science and Technology Corporation (JST); by Research on Neurodegenerative Diseases, Health Science Research Grants from the Ministry of Health, Labor and Welfare; and a Grant-in-Aid for Research on Specific Diseases from the Ministry of Health, Labor and Welfare of Japan.

References

Alisky, J.M., Davidson, B.L., 2000. Gene therapy for amyotrophic lateral sclerosis and other motor neuron diseases. Hum. Gene Ther. 11, 2315–2329.

Bueler, H., 1999. Adeno-associated viral vectors for gene transfer and gene therapy. Biol. Chem. 380, 613–622.

Chirumle, N., Xiao, W., Truneh, A., Schnell, M.A., Hughes, J.V., Zoltick, P., Wilson, J.M., 2000. Humoral immunity to adeno-associated virus type 2 vectors following administration to murine and nonhuman primate muscle. J. Virol. 74, 2420–2425.

Distefano, P.S., 1993. Neurotrophic factors in the treatment of motor neuron disease and trauma. Exp. Neurol. 124, 56–59.

Henderson, C.E., Phillips, H.S., Pollock, R.A., Davies, A.M., Lemeulle, C., Armanini, M., Simmons, L., Moffet, B., Vandlen, R.A., Simpson, L.C., 1994. GDNF: a potent survival factor for motoneurons present in peripheral nerves and muscle. Science 266, 1062–1064.

Jing, S., Wen, D., Yu, Y., Holst, P.L., Luo, Y., Fang, M., Tamir, R., Antonio, L., Hu, Z., Cupples, R., Louis, J.C., Hu, S., Altrock, B.W., Fox, G.M., 1996. GDNF-induced activation of the Ret protein tyrosine kinase is mediated by GDNFR-α, a novel receptor for GDNF. Cell 85, 1113–1124.

Kaspar, B.K., Erickson, D., Schaffer, D., Hinh, L., Gage, F.H., Peterson, D.A., 2002. Targeted retrograde gene delivery for neuronal protection. Mol. Ther. 5, 50–56.

Keller-Peck, C.R., Feng, G., Sanes, J.R., Yan, Q., Lichtman, J.W., Snider, W.D., 2001. Glial cell line-derived neurotrophic factor administration in postnatal life results in motor unit enlargement and continuous synaptic remodeling at the neuromuscular junction. J. Neurosci. 21, 6136–6146.

Kirik, D., Rosenblad, C., Bjorklund, A., Mandel, R.J., 2000. Long-term rAAV-mediated gene transfer of GDNF in the rat Parkinson's model: intrastriatal but not intranigral transduction promotes functional regeneration in the lesioned nigrostriatal system. J. Neurosci. 20, 4686–4700.

Kordower, J.H., Emborg, M.E., Bloch, J., Ma, S.Y., Chu, Y., Leventhal, L., Mcbride, J., Chen, E.Y., Palfi, S., Roitberg, B.Z., Brown, W.D., Holden, J.E., Pyzalski, R., Taylor, M.D., Carvey, P., Ling, Z., Trono, D., Hantraye, P., Deglon, N., Aebischer, P., 2000. Neurodegeneration prevented by lentiviral vector delivery of GDNF in primate models of Parkinson's disease. Science 290, 767–773.

Leitner, M.L., Molliver, D.C., Osborne, P.A., Vejsada, R., Golden, J.P., Lampe, P.A., Kato, A.C., Milbrandt, J., Johnson, E.M., Jr, 1999. Analysis of the retrograde transport of glial cell line-derived neurotrophic factor (GDNF), neurturin, and persephin suggests

that in vivo signaling for the GDNF family is GFRalpha coreceptor-specific. J. Neurosci. 19, 9322–9331.

Mandel, R.J., Snyder, R.O., Leff, S.E., 1999. Recombinant adeno-associated viral vector-mediated glial cell line-derived neurotrophic factor gene transfer protects nigral dopamine neurons after onset of progressive degeneration in a rat model of Parkinson's disease. Exp. Neurol. 160, 205–214.

Matsushita, T., Elliger, S., Elliger, C., Podsakoff, G., Villarreal, L., Kurtzman, G.J., Iwaki, Y., Colosi, P., 1998. Adeno-associated virus vectors can be efficiently produced without helper virus. Gene Ther. 5, 938–945.

Mitsuma, N., Yamamoto, M., Li, M., Ito, Y., Mitsuma, T., Mutoh, T., Takahashi, M., Sobue, G., 1999. Expression of GDNF receptor (RET and GDNFR-alpha) mRNAs in the spinal cord of patients with amyotrophic lateral sclerosis. Brain Res. 820, 77–85.

Neet, K.E., Capenot, R.B., 2001. Receptor binding, internalization, and retrograde transport of neurotrophic factors. Cell. Mol. Life Sci. 58, 1021–1235.

Nguyen, Q.T., Parsadanian, A.S., Snider, W.D., Lichtman, J.W., 1998. Hyperinnervation of neuromuscular junctions caused by GDNF overexpression in muscle. Science 279, 1725–1729.

Okragly, A.J., Haak-frendscho, M., 1997. An acid-treatment method for the enhanced detection of GDNF in biological samples. Exp. Neurol. 145, 592–596.

Oppenheim, R.W., Houenou, L.J., Johnson, J.E., Lin, L.F., Li, L., Lo, A.C., Newsome, A.L., Prevette, D.M., Wang, S., 1995. Developing motoneurons rescued from programmed and axotomy-induced cell death by GDNF. Nature 373, 344–346.

Rabinowitz, J.E., Samulski, J., 1998. Adeno-associated virus expression systems for gene transfer. Curr. Opin. Biotechnol. 9, 470–475.

Suzuki, H., Hase, A., Miyata, Y., Arahata, K., Akazawa, C., 1998. Prominent expression of glial cell line-derived neurotrophic factor in human skeletal muscle. J. Comp. Neurol. 402, 303–312.

Tomac, A., Widenfalk, J., Lin, L.F., Kohno, T., Ebendal, T., Hoffer, B.J., Olson, L., 1995. Retrograde axonal transport of glial cell line-derived neurotrophic factor in the adult nigrostriatal system suggests a trophic role in the adult. Proc. Natl. Acad. Sci. USA 92, 8274–8278.

Verma, I.M., Somia, N., 1997. Gene therapy—promises, problems and prospects. Nature 389, 239–242.

Wang, L., Muramatsu, S., Lu, Y., Ikeguchi, K., Fujimoto, K., Okada, T., Mizukami, H., Hanazono, Y., Kume, A., Urano, F., Ichinose, H., Nagatsu, T., Nakano, I., Ozawa, K., 2002a. Delayed delivery of AAV-GDNF prevents nigral neurodegeneration and promotes functional recovery in a rat model of Parkinson's disease. Gene Ther. 9, 381–389.

Wang, L.J., Lu, Y.Y., Muramatsu, S., Ikeguchi, K., Fujimoto, K., Okada, T., Mizukami, H., Matsushita, T., Hanazono, Y., Kume, A., Nagatsu, T., Ozawa, K., Nakano, I., 2002b. Neuroprotective effects of glial cell line-derived neurotrophic factor mediated by an adeno-associated virus vector in a transgenic animal model of amyotrophic lateral sclerosis. J. Neurosci. 22, 6920–6928.

Yamamoto, M., Mitsuma, N., Inukai, A., Ito, Y., Li, M., Mitsuma, T., Sobue, G., 1999. Expression of GDNF and GDNFR-alpha mRNAs in muscles of patients with motor neuron diseases. Neurochem. Res. 24, 785–790.

Yan, Q., Matheson, C., Lopez, O.T., 1995. In vivo neurotrophic effects of GDNF on neonatal and adult facial motoneurons. Nature 373, 341–344.

Yuen, E.C., 2001. The role of neurotrophic factors in disorders of peripheral nerves and motor neurons. Phys. Med. Rehabil. Clin. North Am. 12, 293–306.

Gene Therapy (2003) 10, 51–58

www.nature.com/gt

RESEARCH ARTICLE

Suicide gene therapy using AAV-HSVtk/ganciclovir in combination with irradiation results in regression of human head and neck cancer xenografts in nude mice

T Kanazawa[1,2,3], H Mizukami[1,3], T Okada[1,3], Y Hanazono[1,3], A Kume[1,3], H Nishino[2], K Takeuchi[4], K Kitamura[5], K Ichimura[2] and K Ozawa[1,3,6]

[1]*Division of Genetic Therapeutics, Center for Molecular Medicine, Jichi Medical School, Tochigi, Japan;* [2]*Department of Otolaryngology, Jichi Medical School, Tochigi, Japan;* [3]*CREST, Japan Science and Technology Corporation (JST), Tochigi, Japan;* [4]*Department of Anatomy, Jichi Medical School, Tochigi, Japan;* [5]*Department of Otolaryngology, School of Medicine, Tokyo Medical and Dental University, Tokyo, Japan ; and* [6]*Department of Hematology, Jichi Medical School, Tochigi, Japan*

The application of adeno-associated virus (AAV) vectors to cancers is limited by their low transduction efficiency. Previously, we reported that γ-ray enhanced the second-strand synthesis, leading to the improvement of the transgene expression, and cytocidal effect of the herpes simplex virus type-1 thymidine kinase (HSVtk) and ganciclovir (GCV) system. In this study, we extended this in vitro findings to in vivo. First, the laryngeal cancer cell line (HEp-2) and HeLa were treated with AAVtk/GCV, the number of surviving cells was reduced as the concentration of GCV increased. Furthermore, the 4 Gy irradiation enhanced the killing effects of AAVtk/GCV by four-fold on HeLa cells and 15-fold on HEp-2 cells. Following the in vitro experiments, we evaluated the transgene expression and the antitumor activity of the AAV vectors in combination with γ-ray in nude mice inoculated with HEp-2 subcutaneously. The LacZ expression was observed in the xenografted tumors and significantly increased by γ-ray. The AAVtk/GCV system suppressed the tumors growth, and γ-ray augmented the antitumor activity by five-fold. These findings suggest that the combination of AAVtk/GCV system with radiotherapy is significantly effective in the treatment of cancers and may lead to reduction of the potential toxicity of both AAVtk/GCV and γ-ray.

Gene Therapy (2003) **10**, 51–58. doi:10.1038/sj.gt.3301837

Keywords: *adeno-associated virus vector; herpes simplex thymidine kinase; irradiation; animal experiments; head and neck neoplasms*

Introduction

Current therapy for the head and neck cancer utilizes an aggressive multimodal approach with surgery, radiotherapy, and chemotherapy, depending on the tumor stage and patient characteristics. Despite advances in the therapeutic approaches, no substantial improvement in efficacy and survival has occurred over the past several decades. Conventional palliative treatments, such as chemotherapy, are often toxic and sometimes ineffective. In addition, no effective salvage therapy is available for whom standard treatment fails. Therefore, new treatments are needed both to improve survival in the long term and to obtain worthwhile, less toxic palliation in the short term.

Recent progress in gene therapy technologies has made it possible to develop novel therapeutic strategies for intractable cancers. Head and neck cancer is particularly well suited for gene transduction strategies. First, its location in the upper aerodigestive tract allows easy access for vector delivery and assessment of response. Second, targeting of gene transduction can be achieved by direct injection of the vector into the tumor. Finally, metastases mostly occur late in head and neck cancer progression, making local disease responsible for most of the morbidity and mortality.[1,2] Therefore, any improvement in local disease control implies benefits for patients. At present, several virus vectors such as retroviral, adenoviral and adeno-associated virus (AAV) vectors[3,4] have been utilized for the experiments of cancer gene therapy. AAV is a non-pathogenic virus with a single-stranded DNA genome.[5,6] AAV vectors have emerged as a useful alternative to other vectors,[7] and AAV have been evaluated in preclinical and clinical models for cystic fibrosis,[8] Parkinson's disease[9] and Hemophilia B.[10] AAV vectors have a broad host range and can transduce head and neck cancer cells.[11] However, an obstacle to these applications is a low transgene expression efficiency, mainly due to a limited second-strand synthesis.[12,13] Recently, γ-ray irradiation has been reported to enhance the second-strand synthesis of the AAV vector genome and improve the transgene expression.[14–16] In our previous study, we demonstrated that γ-rays enhance AAV-mediated transgene expression in maxillary sinus cancer cells *in vitro*.[11] Thus, an AAV

Correspondence: K Ozawa, Division of Genetic Therapeutics, Center for Molecular Medicine, Jichi Medical School, 3311-1 Yakushiji Minamikawachi, Tochigi 329-0498, Japan
Received 15 January 2002; accepted 10 June 2002

vector encoding suicide gene would kill target cells more efficiently when combined with γ-ray irradiation therapy. Although the herpes simplex virus type-1 thymidine kinase (HSVtk)/ganciclovir (GCV) system has shown to be effective for controlling tumor growth in animal models,[17–20] this therapeutic approach alone sometimes fails to eradicate cancer cells, and tumors recur thereafter. Thus, alternative therapeutic modalities, such as combination therapy should be considered.[21,22]

In this study, we demonstrate effective suicide gene therapy using the AAV vector in combination with γ-ray irradiation, enhancing the antitumor activity both *in vitro* and *in vivo*.

Results

Comparison of the transduction efficiency of AAVLacZ between HeLa and HEp-2 cells

HeLa or HEp-2 cells were transduced with recombinant AAV with *Escherichia coli* LacZ expression cassette (AAVLacZ) at titers from 1×10^4 to 1×10^6 particles/cell (Figure 1a). The percentage of positive HEp-2 cells for 5-bromo-4-chloro-indonyl-β-D-galactopyranoside (X-gal) staining reached 72% when the cells were transduced with 1×10^6 particles/cell of AAVLacZ. The transduction efficiency of HEp-2 cells was almost as high as that of HeLa cells. Figure 1b shows the β-galactosidase expression level in HeLa and HEp-2 cells quantified by enzyme-linked immunosorbent assay (ELISA), when the cells were transduced with AAVLacZ at titers from 1×10^3 to 1×10^5 particles/cells. The amount of β-gal in both cells increased along with the increased concentration of AAVLacZ.

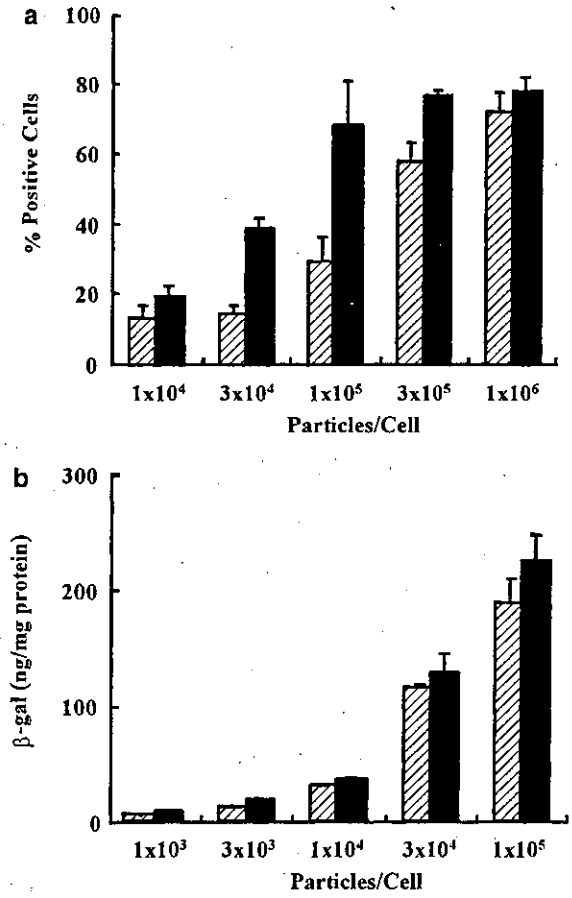

Figure 1 AAVLacZ expression in HeLa or HEp-2 cells. (a) Subconfluent HeLa (closed bar) or HEp-2 cells (hatched bar) were transduced with AAVLacZ at various doses ranging from 1×10^4 to 1×10^6 particles/cell. At 36 h post-transduction, the cells were fixed and stained with X-gal, and then positive cells were counted. (b) Subconfluent HeLa (closed bar) or HEp-2 cells (hatched bar) were transduced with 1×10^3 to 1×10^5 particles/cell of AAVLacZ. Thirty-six hours after transduction, the cells were lysed and β-gal was assayed by using the β-gal ELISA kit. Each bar represents the mean ± s.d.

Effect of γ-ray irradiation on AAV-mediated transgene expression

γ-Rays have been shown to increase the transduction efficiency with AAV vectors, mainly by accelerating the rate of leading-strand synthesis of the AAV vector genome. According to our previous study,[11] optimal transduction efficiency was obtained when the cells were transduced with 1×10^3 particles/cell of AAVLacZ immediately after irradiation. In Figure 2, γ-ray irradiation significantly increased LacZ expression in HeLa and HEp-2 cells in a dose-dependent manner. (one-way ANOVA: $P < 0.01$).

γ-Rays enhance the second-strand synthesis of the AAV genome in HeLa and HEp-2 cells

To examine whether the second-strand synthesis of the AAV vector genome occurs more efficiently in γ-ray-irradiated cells, HeLa and HEp-2 cells were subjected to

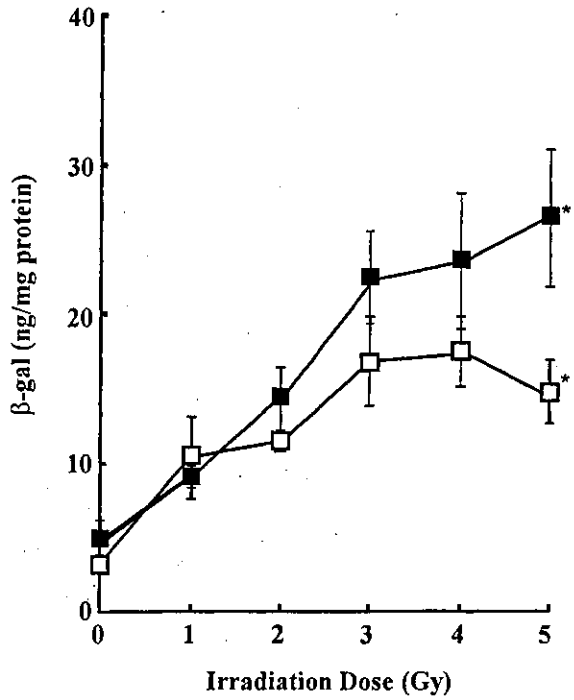

Figure 2 Effect of γ-ray on AAV vector-mediated transgene expression. HeLa (closed square) or HEp-2 cells (open square) were transduced with 1×10^3 particles/cell of AAVLacZ immediately after γ-ray irradiation at doses ranging from 0 to 5 Gy. Thirty-six hours after transduction, the expression levels of LacZ were assayed by using the β-gal ELISA kit. Data were statistically analyzed by one-way ANOVA ($P < 0.01$). Each data point represents the mean ± s.d.*

0, 2, or 4 Gy of γ-ray irradiation, and then transduced with 1×10^4 particles/cell of AAVLacZ. Forty-eight hours after transduction, total DNA was isolated, treated with mung bean nuclease, and then loaded on 1% agarose gels. After transfer to nylon membranes, signals corresponding to the AAVLacZ genome were detected (Figure 3). Mung bean nuclease was used to digest the single-stranded DNA and to clearly visualize the double-stranded replicative form (RF) of the AAV vector genome. The RF was almost equal to 4.7 kb fragment derived from pAAVLacZ in size. At the dose of 4 Gy, in both HeLa and HEp-2 cells, the intensity of signal corresponding to the RF increased significantly, suggesting that the augmented transgene expression was associated with the conversion of the AAV vector genome to the double-stranded RF.

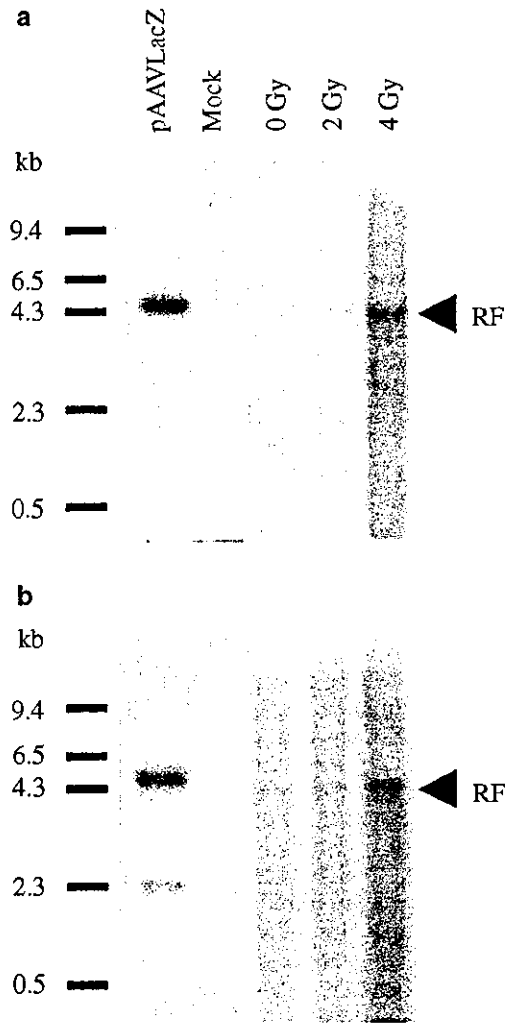

Figure 3 Second-strand synthesis of AAVLacZ genome after γ-ray irradiation in HeLa or HEp-2 cells. HeLa (a) or HEp-2 cells (b) were transduced with 1×10^4 particles/cell of AAVLacZ immediately after 0, 2, or 4 Gy of γ-ray irradiation. Two days later, total DNA was isolated in a low-salt condition. After mung bean nuclease treatment, the DNA samples were loaded on 1% agarose gels, transferred onto nylon membranes (Hybond N⁺, Amersham), and then hybridized with a radiolabeled CMV-specific probe. Signals were detected by using an imaging analyzer. Lane 1, a 4.7 kb fragment derived from pAAVLacZ; lane 2, mock transduced; lanes 3–5, AAVLacZ-transduced immediately after 0-, 2-, or 4-Gy irradiation respectively. RF: the double-stranded replicative form.

GCV treatment

Figure 4 shows the killing effect of various concentrations of GCV on HeLa and HEp-2 cells transduced with 1×10^5 particles/cell of recombinant AAV with HSVtk expression cassette (AAVtk) (closed bar). When the AAVtk-transduced cells were treated with 1 μg/ml of GCV, 75% of HeLa cells and 35% of HEp-2 cells were killed. As the concentration of GCV was increased, surviving cells were reduced and 98% of HeLa cells and 96% of HEp-2 cells were killed by exposure to 10 μg/ml of GCV, which was significantly higher than the killing rate in AAVLacZ-transduced cells (hatched bar) or mock-transduced cells (open bar) (two-way ANOVA: $P<0.01$).

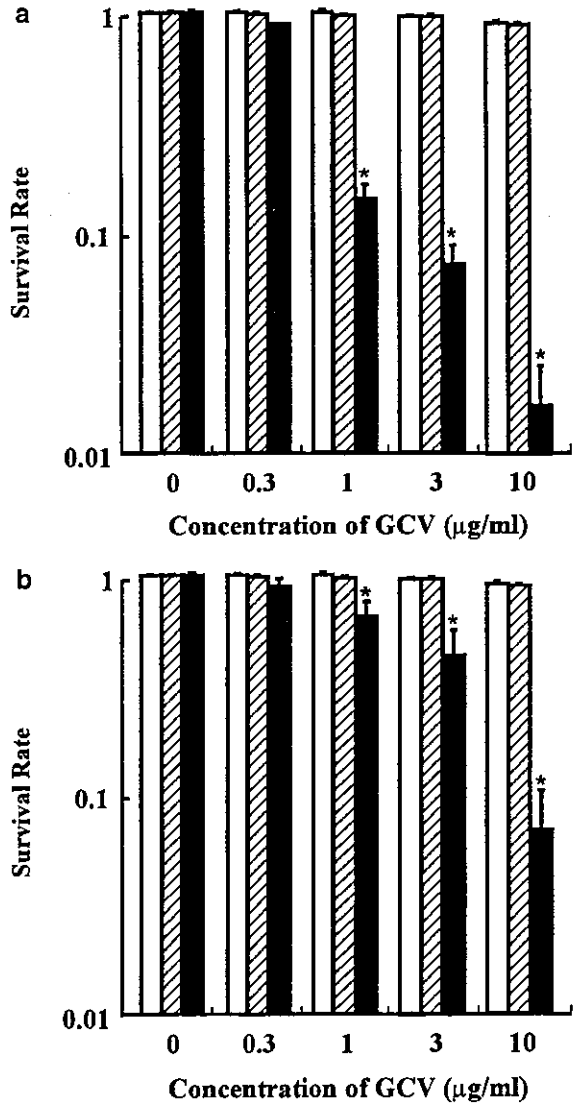

Figure 4 Survival of HeLa and HEp-2 cells upon AAVtk/GCV. HeLa (a) or HEp-2 cells (b) were mock transduced (open bar), transduced with 1×10^5 particles/cell of AAVLacZ (hatched bar), or AAVtk (closed bar). Twenty-four hours after transduction, the cells were exposed to different concentrations of GCV. After a 7-day incubation in the presence of GCV, surviving cells were counted. Data were analyzed by two-way ANOVA. Asterisks mean that the data obtained for AAVtk transduction were significantly different from those with or without transduction of AAVLacZ ($P<0.01$). Each bar represents the mean ± s.d. ($n=3$).

Enhanced cytocidal effect of the AAVtk/GCV system by γ-ray irradiation

To facilitate comparison of the therapeutic outcome, the killing effect of GCV (3 μg/ml) on HeLa or HEp-2 cells transduced with various doses of AAVtk with or without γ-ray irradiation was evaluated (Figure 5). When HeLa and HEp-2 cells were transduced with 3×10^4 particles/cell of AAVtk without irradiation, 48% of the HeLa cells and 40% of the HEp-2 cells were killed by the exposure to the GCV. As the dose of AAVtk was increased, the number of surviving cells were reduced, and 98% of the HeLa cells and 95% of the HEp-2 cells were killed when transduced with 3×10^5 particles/cell of AAVtk, which was significantly higher than the killing rate in the case of AAVLacZ-transduced cells as expected. To investigate whether γ-ray enhances the killing effect of AAVtk/GCV, HeLa and HEp-2 cells were irradiated with 2 or 4 Gy of γ-ray immediately before the transduction with various doses of AAVtk, and then cultured in 3 μg/ml of GCV. When the HeLa cells were transduced with 3×10^4 particles/cell of AAVtk, 70% of the 2 Gy irradiated cells and 85% of the 4 Gy irradiated cells were killed by the addition of GCV. When the HeLa cells were transduced at 3×10^5 particles/cell, γ-ray irradiation enhanced the killing effects of AAVtk/GCV system by four-fold. γ-Ray irradiation also enhanced the killing effects on HEp-2 cells by 15-fold. The enhancement by γ-ray irradiation was calculated from the ratio of 4 Gy irradiated survival rate to non-irradiated survival rate. These results show that γ-ray irradiation enhances the killing effects of AAVtk/GCV system significantly (two-way ANOVA: $P<0.01$).

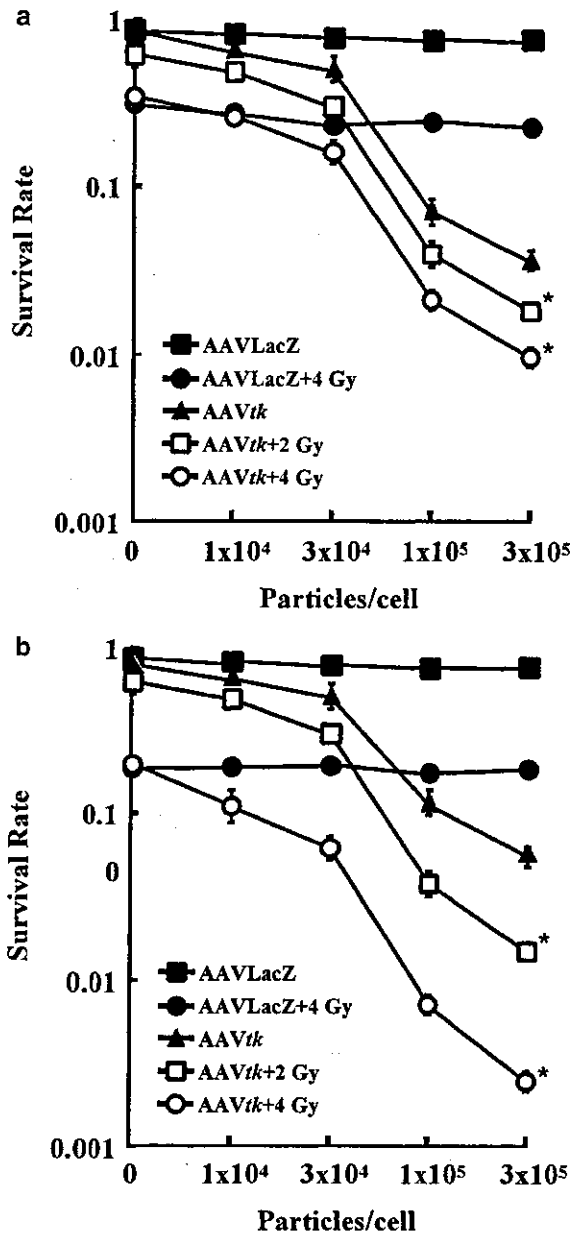

Figure 5 Enhancement of the cytocidal effect of AAVtk by γ-ray irradiation. HeLa (a) or HEp-2 cells (b) were transduced with various doses of AAVLacZ or AAVtk with or without γ-ray irradiation. Twenty-four hours after transduction, the cells were treated with 3 μg/ml of GCV. After a 7-day incubation in the presence of GCV, surviving cells were counted. Closed squares: AAVLacZ-transduced cells; closed circles: AAVLacZ-transduced cells with 4 Gy irradiation; closed triangles: AAVtk-transduced cells; open squares: AAVtk-transduced cells with 2 Gy irradiation; open circles: AAVtk-transduced cells with 4 Gy irradiation. Asterisks mean that the AAVtk-transduced and irradiated cells were significantly different from the AAVtk-transduced and non-irradiated cells ($P<0.01$). Each data point represents the mean ± s.d.

γ-Ray enhances the transgene expression in vivo

To assess the enhancement of transgene expression by γ-ray irradiation *in vivo*, the AAVLacZ-transduced tumors were stained with X-gal (Figure 6). Compared with non-irradiated control, the tumors irradiated at 4 Gy showed increased number of X-gal-positive cells. To quantify the amount of β-galactosidase, we homogenized the non-irradiated or 4 Gy irradiated tumors and measured with the β-gal ELISA kit. As shown in Figure 7, the amount of β-galactosidase in 4 Gy irradiated tumors was 2.5 times larger than that in non-irradiated tumors (one-way ANOVA: $P<0.01$).

Suppressive effects of combination therapy upon tumor growth in vivo

To examine the killing effect of this system *in vivo*, tumor nodules were established in the flanks of BALB/c nude mice by subcutaneous injection of the HEp-2 cells. Once tumors were established, those animals were irradiated at 4 Gy and then directly injected with 1×10^{12} particles of AAVLacZ or AAVtk in the tumors. Administration of GCV (50 mg/kg) or phosphate-buffered saline (PBS) intraperitoneally twice a day was started at 24 h after the vector injection and continued for 2 weeks. The tumors were measured every 3 days.

Five treatment groups of 4 or 5 animals each were established: Group 1 is the AAVLacZ-transduced animals with PBS administration (n=4). Group 2 is the AAVtk-transduced animals with GCV administration (n=5). Group 3 is the AAVLacZ-transduced animals with 4 Gy irradiation and GCV administration (n=5). Group 4 is the AAVtk-transduced animals with 4 Gy irradiation and PBS administration (n=4). Group 5 is the AAVtk-transduced animals with 4 Gy irradiation and GCV administration.

The representative growth curve of the tumors after treatment is shown in Figure 8. The AAVtk/GCV system suppressed the growth rate of xenografted tumors by